

Aisaki K, Aizawa S, Fujii H, Kanno J, Kanno H	Glycolytic inhibition by mutation of pyruvate kinase gene increases oxidative stress and causes apoptosis of a pyruvate kinase deficient cell line.	Exp Hematol	35	1190 - 1200	2007
Nakatsu N, Nakamura T, Yamazaki K, Sadahiro S, Makuuchi H, Kanno J, Yamori T.	Evaluation of action mechanisms of toxic chemicals using JFCR39, a panel of human cancer cell lines.	Mol Pharmacol.	72	1171 - 1180	2007
Grun F, Watanabe H, Zamanian Z, Maeda L, Arima K, Chubacha R, Gardiner DM, Kanno J, Iguchi T, Blumberg B	Endocrine disrupting organotin compounds are potent inducers of adipogenesis in vertebrates	Mol Endocrinol	20	2141 - 2155	2006
Watanabe Y, Kokubo H, Miyagawa-Tomita S, Endo M, Igarashi K, Aisaki KI, Kanno J, Saga Y	Activation of Notch1 signaling in cardiogenic mesoderm induces abnormal heart morphogenesis in mouse	Development	133	1625 - 1634	2006
Nakamura Y, Suzuki T, Igarashi K, Kanno J, Furukawa T, Tazawa C, Fujishima F, Mura I, Ando T, Moriyama N, Moriya T, Saito H, Yamada S, Sasano H	PTOVI: a novel testosterone-induced atherogenic gene in human aorta.	Pathol	209	522 - 531	2006
Kanno J, Aisaki K, Igarashi K, Nakatsu N, Ono A, Kodama Y, Nagao T	"Per cell" normalization method for mRNA measurement by quantitative PCR and microarrays	BMC Genomics	7	64	2006
Shiina H, Matsumoto T, Sato T, Igarashi K, Miyamoto J, Takemasa S, Sakari M, Takada I, Nakamura T, Metzger D, Chambon P, Kanno J, Yoshikawa H, Kato S	Premature ovarian failure in androgen receptor-deficient mice	Proc Natl Acad Sci U S A	103	224 - 229	2006

# Estrogen Prevents Bone Loss via Estrogen Receptor $\alpha$ and Induction of Fas Ligand in Osteoclasts

Takashi Nakamura,<sup>1,2,9</sup> Yuuki Imai,<sup>1,3,9</sup> Takahiro Matsumoto,<sup>1,2</sup> Shingo Sato,<sup>4</sup> Kazusane Takeuchi,<sup>1</sup> Katsuhide Igarashi,<sup>5</sup> Yoshifumi Harada,<sup>6</sup> Yoshiaki Azuma,<sup>6</sup> Andree Krust,<sup>7</sup> Yoko Yamamoto,<sup>1</sup> Hiroshi Nishina,<sup>4</sup> Shu Takeda,<sup>4</sup> Hiroshi Takayanagi,<sup>4</sup> Daniel Metzger,<sup>7</sup> Jun Kanno,<sup>5</sup> Kunio Takaoka,<sup>3</sup> T. John Martin,<sup>8</sup> Pierre Chambon,<sup>7</sup> and Shigeaki Kato<sup>1,2,\*</sup>

<sup>1</sup>Institute of Molecular and Cellular Biosciences, University of Tokyo, Yayoi 1-1-1, Bunkyo-ku, Tokyo 113-0032, Japan

<sup>2</sup>Exploratory Research for Advanced Technology, Japan Science and Technology Agency, Honcho 4-1-8, Kawaguchi, Saitama 332-0012, Japan

<sup>3</sup>Department of Orthopaedic Surgery, Osaka City University Graduate School of Medicine, Asahimachi 1-4-3, Abeno-ku, Osaka, 545-8585, Japan

<sup>4</sup>Tokyo Medical and Dental University, Yushima 1-5-45, Bunkyo-ku, Tokyo 113-8510, Japan

<sup>5</sup>Division of Cellular and Molecular Toxicology, National Institute of Health Sciences, 1-18-1 Kamiyoga, Setagaya-ku, Tokyo 158-8501, Japan

<sup>6</sup>Teijin Institute for Biomedical Research, Asahigaoka 4-3-2, Hino, Tokyo 191-8512, Japan

<sup>7</sup>Institut de Génétique et de Biologie Moléculaire et Cellulaire, Département de Physiological Genetics / Inserm, U-596 / CNRS, UMR7104 / Université Louis Pasteur, Illkirch, Strasbourg, F-67400 France

<sup>8</sup>St. Vincent's Institute of Medical Research, 9 Princes Street, Fitzroy VIC 3065, Australia

<sup>9</sup>These authors contributed equally to this work.

\*Correspondence: uskato@mail.ecc.u-tokyo.ac.jp

DOI 10.1016/j.cell.2007.07.025

## SUMMARY

Estrogen prevents osteoporotic bone loss by attenuating bone resorption; however, the molecular basis for this is unknown. Here, we report a critical role for the osteoclastic estrogen receptor  $\alpha$  (ER $\alpha$ ) in mediating estrogen-dependent bone maintenance in female mice. We selectively ablated ER $\alpha$  in differentiated osteoclasts (ER $\alpha^{\Delta Oc/\Delta Oc}$ ) and found that ER $\alpha^{\Delta Oc/\Delta Oc}$  females, but not males, exhibited trabecular bone loss, similar to the osteoporotic bone phenotype in postmenopausal women. Further, we show that estrogen induced apoptosis and upregulation of Fas ligand (FasL) expression in osteoclasts of the trabecular bones of WT but not ER $\alpha^{\Delta Oc/\Delta Oc}$  mice. The expression of ER $\alpha$  was also required for the induction of apoptosis by tamoxifen and estrogen in cultured osteoclasts. Our results support a model in which estrogen regulates the life span of mature osteoclasts via the induction of the Fas/FasL system, thereby providing an explanation for the osteoprotective function of estrogen as well as SERMs.

## INTRODUCTION

Bone remodeling is a dynamic metabolic process. The destruction or "resorption" of pre-existing bone by mature osteoclasts is followed by the formation of new bone by osteoblasts. Osteoblasts are derived from pleiotropic mesenchymal stem cells in the bone marrow. Mature osteoclasts are multinuclear, macrophage-like cells, derived from hematopoietic stem cells also in the bone marrow. Bone resorption and deposition are tightly coupled, and their balance defines both bone mass as well as quality. The regulation of bone remodeling is complex. A number of systemic hormones and transcription factors directly regulate the proliferation and differentiation of osteoblasts and osteoclasts (Karsenty, 2006; Karsenty and Wagner, 2002; Rodan and Martin, 2000; Teitelbaum and Ross, 2003). Additionally, the indirect cellular communication among groups of bone cells is also physiologically critical for bone growth and remodeling (Martin and Sims, 2005; Mundy and Elefteriou, 2006). The molecular and genetic mechanisms governing bone cell fate have been intensively studied; however, how the life span of bone cells is determined on a molecular level remains elusive.

Estrogen is a key hormone in bone remodeling in several species. The osteoprotective action of estrogen is demonstrable in rodents and is clinically important in humans, particularly older women (Chien and Karsenty, 2005;

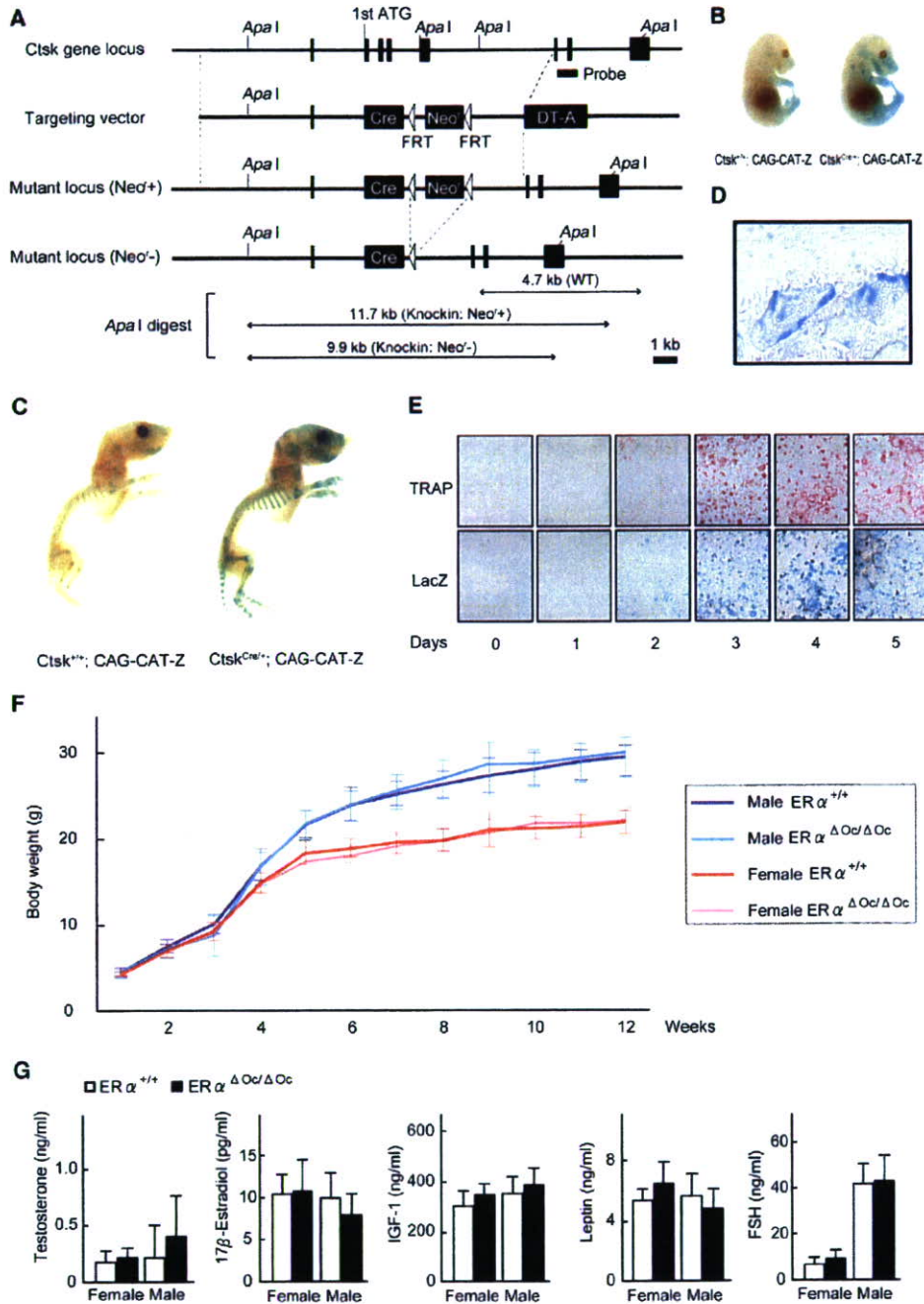


**Figure 1. Generation of Knockin Mice Selectively Expressing Cre in Mature Osteoclasts**

(A) Illustration of the targeting strategy for insertion of the *Cre* gene into the mouse *Cathepsin K* (*Ctsk*) gene. A targeting vector was generated to contain the *Cre* cDNA at the endogenous ATG start site, followed by a *FRT* (Fip-recombinase target)-flanked *Neoc* cassette. The *DT-A* (diphtheria toxin-A) gene was also inserted to avoid random integrations.

(B and C) *Ctsk-Cre* mice were then crossed with CAG-CAT-Z mice.  $\beta$ -galactosidase activity derived from the activated *LacZ* reporter gene was monitored to test if expressed Cre excised the *loxP* sites in mature osteoclasts. LacZ expression patterns reflected the localization patterns of mature osteoclasts in the developing bone at 16.5 days post coitum embryos and in the skeletal tissues of 7-day-old pups.

(D) The LacZ expression induced by Cre-mediated excision was also seen in osteoclasts attached to trabecular bone in the lumbar vertebrae of 12-week-old mice.

(E) LacZ expression was induced during osteoclastogenesis. Osteoclast-like cells that differentiated from bone-marrow macrophages following culture in the presence of M-CSF and RANKL were stained with TRAP (tartrate-resistant acid phosphatase), a mature osteoclast marker.

Delmas, 2002; Raisz, 2005; Rodan and Martin, 2000). Estrogen deficiency in postmenopausal women frequently leads to osteoporosis, the most common skeletal disorder. Similarly, ovariectomy clearly produces an osteoporotic bone phenotype in mice. Osteoporotic bone loss is the result of high bone turnover in which bone resorption outpaces bone deposition (Rodan and Martin, 2000; Teitelbaum, 2007). This imbalance in bone turnover that is induced by estrogen deficiency in women and female rodents can be ameliorated with bio-available estrogens including selective estrogen receptor modulators (SERMs) (Riggs and Hartmann, 2003).

Estrogen and SERMs primarily act by regulating gene transcription via estrogen receptors (ER $\alpha$ , ER $\beta$ ) (Couse and Korach, 1999; Shang and Brown, 2002). ERs belong to the nuclear receptor gene superfamily and act as ligand-inducible transcriptional factors (Mangelsdorf et al., 1995). ER dimers directly or indirectly associate with specific DNA elements in the target gene promoter (Shang and Brown, 2002) and control transcription through reorganizing chromatin structure and histone modifications (Belandria and Parker, 2003). Genetic mouse models (KO mice) lacking ER $\alpha$  (ER $\alpha^{-/-}$ ) and ER $\beta$  (ER $\beta^{-/-}$ ) provide insights into ER function (Mueller and Korach, 2001; Windahl et al., 2002). In mice, though ER $\alpha$  appears to be the major receptor in most estrogen target tissues including bone (Sims et al., 2003), neither clear bone loss nor high bone turnover is detectable in ER $\alpha$  single or ER $\alpha$ /ER $\beta$  double-KO females (Syed and Khosla, 2005; Windahl et al., 2002). This unexpected maintenance of bone mass in female mutants is presumed to be due to unphysiologically elevated levels of other osteoprotective hormones, like androgens. Systemic defects in the hypothalamus caused by ER inactivation appear to impair the negative feedback system of hormone production (Syed and Khosla, 2005). This leads to an excess in estrogen precursors, notably androgens. In fact, the anabolic effects of androgens mediated by the androgen receptor (AR) are evident in female mice (Kawano et al., 2003; Sims et al., 2003). In males, estrogen is also osteoprotective, as is evident by the development of osteopenia in male patients genetically deficient in ER $\alpha$  (Smith et al., 1994) or aromatase activity (Simpson and Davis, 2001). Thus, irrespective of the accumulating clinical and basic research data on the osteoprotective actions of estrogen and SERMs, the molecular basis of this osteoprotection in females remains elusive.

To study the molecular interactions behind the antibone resorptive actions of estrogen in women and female animals, we genetically ablated ER $\alpha$  in mature osteoclasts (ER $\alpha^{\Delta Oc/\Delta Oc}$ ). Selective ablation of ER $\alpha$  in differentiated osteoclasts (ER $\alpha^{\Delta Oc/\Delta Oc}$ ) was accomplished by crossing a *Cathepsin K-Cre* knockin mouse with a floxed ER $\alpha$  mouse. This resulted in clear trabecular bone loss and

high bone turnover associated with increased osteoclast numbers in females but not in males. In the female mutants, further bone loss following ovariectomy was not significant and recovery by estrogen was ineffective in the trabecular areas of long bones and lumbar vertebral bodies. Upregulated expression of *Fas ligand* (*FasL*) gene, and increased apoptosis in differentiated osteoclasts by estrogen was found in the intact bone of wild-type females but undetectable in ER $\alpha^{\Delta Oc/\Delta Oc}$  females. Induction of FasL and apoptosis by estrogen as well as a SERM also required ER $\alpha$  in cultured osteoclasts. Thus, we propose that the osteoprotective actions of estrogen and SERMs are mediated at least in part through osteoclastic ER $\alpha$  in trabecular bone, and the life span of mature osteoclasts is regulated through the activation of the FasL signaling.

## RESULTS

### Generation of Osteoclast-Specific ER $\alpha$ Gene Disruption by Knocked-In Cre in the *Cathepsin K* Gene

To specifically disrupt ER $\alpha$  gene in mature osteoclasts, we knocked in Cre into the gene locus of *Cathepsin K* (*Ctsk*<sup>Cre/+</sup>) (Figures 1A, S1A, and S1B), a gene known to be expressed in differentiated osteoclastic cells arising from hematopoietic stem cells. This gene is functionally indispensable for mature osteoclasts (Saftig et al., 1998). Only one copy appears enough to support normal bone formation and bone turnover, since heterozygous mutant mice of *Cathepsin K* (*Ctsk*<sup>+/-</sup>) have no obvious bone phenotype (Gowen et al., 1999; Li et al., 2006; Saftig et al., 1998). Clear, bone-specific expression of the Cre transcript in the adult *Ctsk*<sup>Cre/+</sup> mice was observed in the tested tissues (Figure S1C). To confirm Cre protein expression, the *Ctsk*<sup>Cre/+</sup> mice were crossed with tester mice (CAG-CAT-Z). These mice were genetically engineered to express  $\beta$ -galactosidase by excision of the transcribed stop sequence in front of the  $\beta$ -galactosidase gene (*LacZ*) in cells expressing Cre (Sakai and Miyazaki, 1997).  $\beta$ -galactosidase expression visualized by LacZ staining was observed in the bones of 16.5 dpc embryos and 7-day-old pups of *Ctsk*<sup>Cre/+</sup>; CAG-CAT-Z mice. Expression patterns were consistent with the appearance and skeletal localization of functionally mature osteoclasts (Figures 1B and 1C). Histochemical staining of LacZ in the lumbar vertebrae of 12-week-old mice was localized in multinuclear osteoclasts (Figure 1D) but not seen in osteoblasts and osteocytes (Figure S1D) and the hypothalamus (Figure S1E). Since *Cathepsin K* gene expression is evident in differentiated osteoclasts (Saftig et al., 1998), we used an in vitro culture cell system to test whether Cre expression was driven by the endogenous promoter that is induced at the time of osteoclast differentiation. Osteoclast-precursor cells derived from bone marrow

(F) The growth curve of ER $\alpha^{\Delta Oc/\Delta Oc}$  mice was indistinguishable from that of the control mice. Data are represented as mean  $\pm$  SEM.

(G) Serum hormone levels were normal in 12-week-old ER $\alpha^{\Delta Oc/\Delta Oc}$  (filled column) versus ER $\alpha^{+/+}$  (open column) mice (n = 10–11 animals per genotype). Data are represented as mean  $\pm$  SEM.

were cytodifferentiated for 1 week in the presence of M-CSF (macrophage colony stimulating factor) and RANKL (receptor activator of NF $\kappa$ B ligand) (Koga et al., 2004). TRAP-positive osteoclasts emerged after 3 days of culture (Figure 1E). The number of TRAP-positive osteoclasts and the number of LacZ-expressing cells simultaneously increased. In the contrast, the LacZ expression was not detected in primary cultured osteoblasts derived from the calvaria (Figure S1F). In view of both our *in vivo* and *in vitro* observations, we conclude that the *Ctsk*<sup>Cre/+</sup> mouse line expresses Cre in differentiated osteoclasts. Moreover, estrogen response in bone mass control was not distinguishable in between *Ctsk*<sup>Cre/+</sup> and *Ctsk*<sup>+/+</sup> mice (Figure S2A).

We then crossed floxed *ER $\alpha$*  mice (Dupont et al., 2000) with *Ctsk*<sup>Cre/+</sup> mice to disrupt *ER $\alpha$*  in differentiated osteoclasts (*ER $\alpha$*  <sup>$\Delta$ Oc/ $\Delta$ Oc</sup>). Excision of the *ER $\alpha$*  gene (Figure S1G) was confirmed by Southern blotting of DNA from adult female and male (data not shown) bone as well as in cultured mature osteoclasts (Figure S1H). No overt differences were observed in the growth curve, reproduction, or tissues for up to 12 weeks of age (Figure 1F) between the *Ctsk*<sup>Cre/+</sup>; *ER $\alpha$* <sup>+/+</sup> (*ER $\alpha$* <sup>+/+</sup>) and the *Ctsk*<sup>Cre/+</sup>; *ER $\alpha$* <sup>flx/flx</sup> (*ER $\alpha$*  <sup>$\Delta$ Oc/ $\Delta$ Oc</sup>) mice, with the exception of the female bones. Serum levels of sex hormones and bone remodeling regulators such as IGF-I, leptin, and follicle-stimulating hormone (Sun et al., 2006; Takeda et al., 2002) appeared unchanged in both male and female *ER $\alpha$*  <sup>$\Delta$ Oc/ $\Delta$ Oc</sup> mice at 12 weeks (Figure 1G).

#### Osteopenia Occurred in Osteoclast-Specific *ER $\alpha$* KO Females But Not Males

The 12-week-old *ER $\alpha$*  <sup>$\Delta$ Oc/ $\Delta$ Oc</sup> females exhibited a clear reduction in bone mineral density (BMD) in the femurs (Figures 2A–2C) and tibiae (data not shown) when compared with *ER $\alpha$* <sup>+/+</sup> mice. Though cortical bone appeared unaffected, trabecular bone loss (Figure 2A) with significant reduction of trabecular bone volume (BV/TV) (Figure 2F) was clearly seen. This is similar to the osteoporotic abnormalities observed in women during natural menopause or following ovariectomy (Delmas, 2002; Tolar et al., 2004). However, unlike men deficient in aromatase or *ER $\alpha$*  activity (Simpson and Davis, 2001; Smith et al., 1994), *ER $\alpha$*  <sup>$\Delta$ Oc/ $\Delta$ Oc</sup> males unexpectedly exhibited no clear bone loss even in the trabecular areas (Figures 2A–2C). In *ER $\alpha$*  <sup>$\Delta$ Oc/ $\Delta$ Oc</sup> females, both the bone-formation rate, estimated by double-calcein labeling (Figure 2D), as well as the bone-resorption rate, estimated from TRAP-positive differentiated osteoclast numbers (Figure 2E), were increased, indicating high bone turnover. Histomorphometric analyses of *ER $\alpha$*  <sup>$\Delta$ Oc/ $\Delta$ Oc</sup> females supported the observation of accelerated bone resorption, as increased numbers of osteoclasts (Oc.S/BS and N.Oc/BS) were observed together with more eroded bone surface (ES/BS in Figure 2F). Bone formation was also enhanced as the rates of mineral apposition (MAR) and bone formation (BFR/BS) were both upregulated without an increase in osteoblast numbers (Ob.S/BS) (Figure 2F). Thus, considering all of these find-

ings, it is conceivable that the increased number of differentiated osteoclasts following *ER $\alpha$*  ablation accelerates bone resorption over formation, leading to bone loss in the trabecular areas.

#### No Further Bone Loss Results from Estrogen Deficiency in *ER $\alpha$* <sup>$\Delta$ Oc/ $\Delta$ Oc</sup> Females

To verify whether osteoclastic *ER $\alpha$*  indeed mediates osteoprotective estrogen actions, estrogen action was investigated by ovariectomy (OVX) of 12-week-old female mice. As expected, OVX in *ER $\alpha$* <sup>+/+</sup> females resulted in significantly reduced BMD particularly in the trabecular bone (Figures 3A and 3B) but not in the cortical bone (Figure 3C). Consistent with previous reports, (Kimble et al., 1995; Teitelbaum and Ross, 2003), estrogen deficiency following OVX upregulated the serum levels of cytokines like TNF $\alpha$  and IL-1 $\alpha$  (Figure 3D). These cytokines enhance bone resorption through stimulation of osteoclastogenesis, leading to the loss of bone mass (Teitelbaum and Ross, 2003). OVX did not further reduce BMD or trabecular bone volume of the femurs of *ER $\alpha$*  <sup>$\Delta$ Oc/ $\Delta$ Oc</sup> females (Figure 3B) nor affect increased number of TRAP-positive osteoclasts (see lower panel in Figure 3A) despite upregulation of serum cytokines. This suggests that the expression of cytokines known to regulate bone resorption is not under the control of osteoclastic *ER $\alpha$* .

#### Estrogen Treatment Failed to Rescue the Osteoporotic Bone Phenotype of *ER $\alpha$* <sup>$\Delta$ Oc/ $\Delta$ Oc</sup> Mice

Estrogen treatment by estrogen pellet implantation (OVX + E2) for 2 weeks after OVX in *ER $\alpha$* <sup>+/+</sup> mice elicited a dramatic increase in bone mass in both the trabecular and cortical areas of the femurs (data not shown) and lumbar vertebral bodies (Figure 4A). Estrogen action during E2 treatment in female mutants (*ER $\alpha$*  <sup>$\Delta$ Oc/ $\Delta$ Oc</sup>) was not as pronounced as in the *ER $\alpha$* <sup>+/+</sup> females (Figures 4A and 4B), and the increase in the trabecular portions of the distal femurs was slight (data not shown). Histomorphometric analysis of the lumbar vertebral bodies (Figure 4B) supported the idea that E2 treatment in the female mutants was not sufficient to suppress accelerated bone resorption. These *in vivo* findings in the *ER $\alpha$*  <sup>$\Delta$ Oc/ $\Delta$ Oc</sup> females suggest that in at least the trabecular areas of the long bones and lumbar vertebral bodies, the osteoprotective estrogen action is primarily mediated via osteoclastic *ER $\alpha$*  inhibiting bone resorption.

To further test this hypothesis, we investigated *ER $\alpha$*  protein expression in mature osteoclasts from trabecular bone. Few reports document osteoclastic expression of *ER $\alpha$*  protein and an estrogen response in both intact animals and in *in vitro* cultured osteoclasts (Bland, 2000). We therefore reasoned that *ER* expression ceases during differentiation into mature cells from primary cultures of osteoclast precursors, similar to that observed in other primary culture cell systems such as avian oviduct cells, in which *ER $\alpha$*  protein expression is drastically decreased during culture (Kato et al., 1989). Using highly sensitive immunohistochemistry, we investigated whether

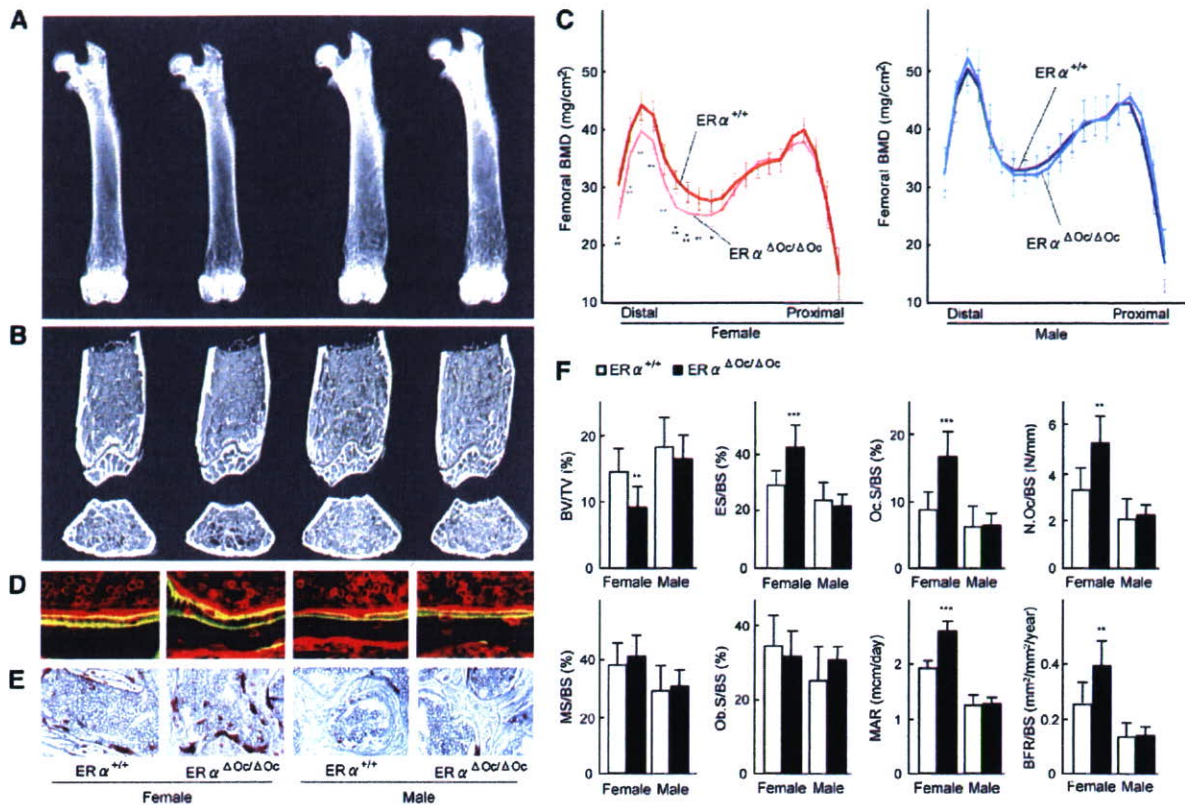


**Figure 2. High Bone Turnover Osteopenia Was Observed in  $ER\alpha^{\Delta Ocl/\Delta Ocl}$  Females But Not Males**

(A) Soft X-ray images of femurs from 12-week-old  $Ctsk^{Cre/+}; ER\alpha^{flax/flax}$  ( $ER\alpha^{\Delta Ocl/\Delta Ocl}$ ) mice.

(B) Three-dimensional computed tomography images of the distal femurs and axial sections of distal metaphysis from representative 12-week-old  $Ctsk^{Cre/+}; ER\alpha^{+/+}$  ( $ER\alpha^{+/+}$ ) and  $ER\alpha^{\Delta Ocl/\Delta Ocl}$  mice.

(C) BMD of each of 20 equal longitudinal divisions of femurs from 12-week-old  $ER\alpha^{+/+}$  and  $ER\alpha^{\Delta Ocl/\Delta Ocl}$  mice. ( $n = 10-11$  animals per genotype; Student's  $t$  test, \* $p < 0.05$ ; \*\* $p < 0.01$ ; \*\*\* $p < 0.001$ ). Data are represented as mean  $\pm$  SEM.

(D) Bone formation was also accelerated in  $ER\alpha^{\Delta Ocl/\Delta Ocl}$  females when two calcein-labeled mineralized fronts visualized by fluorescent microscopy were measured in the proximal tibia of 12-week-old mice.

(E) The number of TRAP-positive osteoclasts in the lumbar spine of female mice was increased by selective disruption of  $ER\alpha$  in osteoclasts, indicating enhanced bone resorption.

(F) Bone turnover parameters as measured by dynamic bone histomorphometry after calcein labeling indicated high bone turnover in  $ER\alpha^{\Delta Ocl/\Delta Ocl}$  females. Parameters are measured in the proximal tibia of 12-week-old  $ER\alpha^{+/+}$  (open column) and  $ER\alpha^{\Delta Ocl/\Delta Ocl}$  (filled column) mice. BV/TV: bone volume per tissue volume. ES/BS: eroded surface per bone surface. Oc.S/BS: osteoclast surface per bone surface. N.Oc/BS: osteoclast number per bone surface. MS/BS: mineralizing surface per bone surface. Ob.S/BS: osteoblast surface per bone surface. MAR: mineral apposition rate. BFR/BS: bone formation rate per bone surface ( $n = 10-11$  animals per genotype; Student's  $t$  test, \* $p < 0.05$ ; \*\* $p < 0.01$ ; \*\*\* $p < 0.001$ ). Data are represented as mean  $\pm$  SEM.

$ER\alpha$  protein expresses in differentiated osteoclasts in the bone tissues of femur sections from 12-week-old mice.  $ER\alpha$  protein expression appeared abundant in osteoblasts and osteocytes of femur sections (Figure 4C) as well as hypothalamus (Figure S2B) from 12-week-old mice, in agreement with a previous report (Zaman et al., 2006). Likewise, expression levels of  $ER\alpha$  in primary cultured osteoblasts derived from calvaria of  $ER\alpha^{\Delta Ocl/\Delta Ocl}$  females appeared unaffected (Figure S2C). In contrast, in differentiated osteoclasts of the same femur sections,  $ER\alpha$  expression was definitely detectable but very low in the  $ER\alpha^{+/+}$  but undetectable in  $ER\alpha^{\Delta Ocl/\Delta Ocl}$  females (Figure 4C).

### Signaling by Osteoclastogenic Factors and Osteoclastogenesis Is Intact in Osteoclasts Deficient in $ER\alpha$

It is possible that the osteoprotective function of osteoclastic  $ER\alpha$  inhibits osteoclastogenesis. To address this issue, osteoclastogenesis was tested in cultured osteoclasts derived from bone-marrow cells of  $ER\alpha^{\Delta Ocl/\Delta Ocl}$  mutants. In this cell culture system, a possible contribution of contaminated immune cells and stromal cells could be excluded, since osteoclastogenesis is only inducible by M-CSF treatment followed by M-CSF + RANKL (Koga et al., 2004).

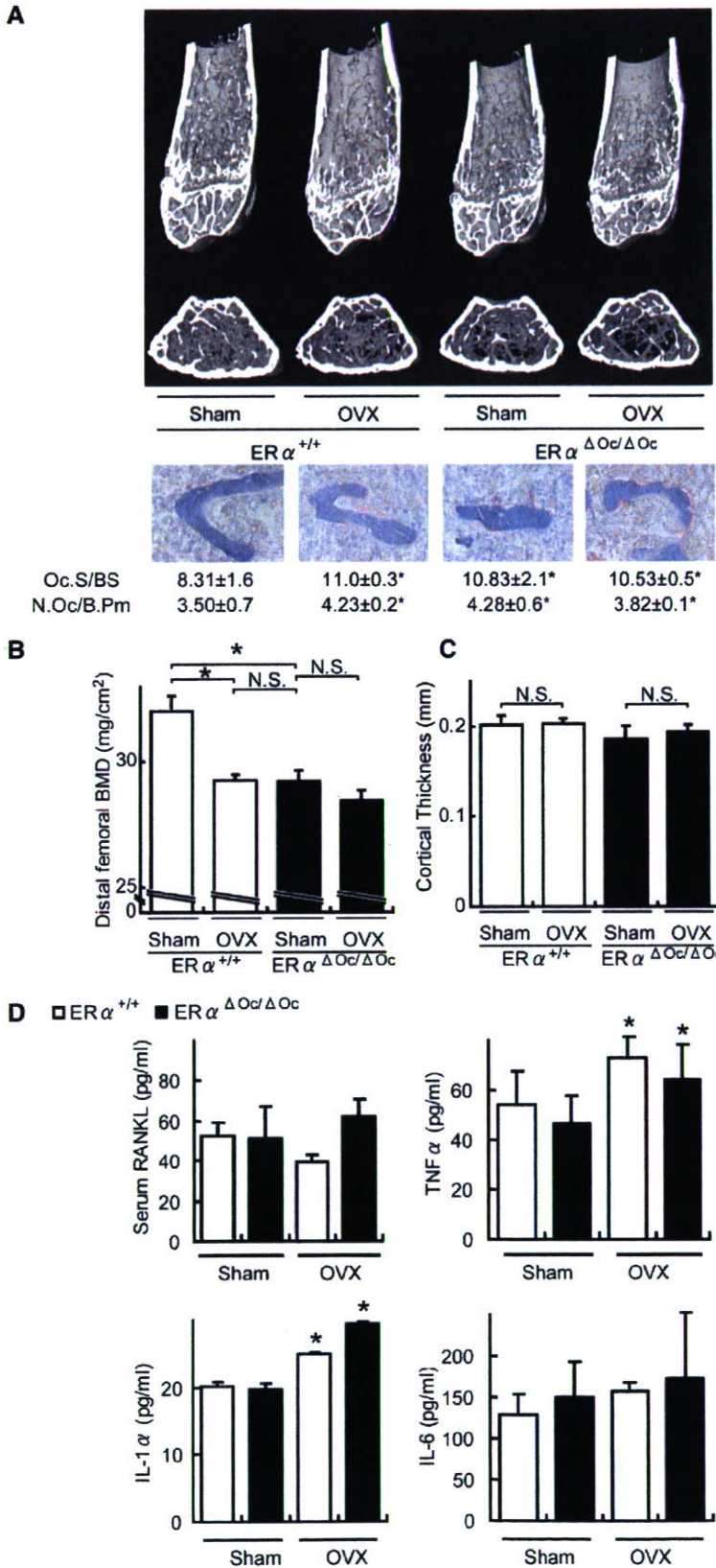


**Figure 3. No Further Bone Loss of  $ER\alpha^{\Delta Oc/\Delta Oc}$  Females by Ovariectomy**

(A) Distal femoral micro CT analysis and lumbar vertebral bone histomorphometrical analysis of sham-operated or ovariectomized (OVX) 12-week-old  $ER\alpha^{+/+}$  and  $ER\alpha^{\Delta Oc/\Delta Oc}$  mice (\* $p < 0.05$  compared to  $ER\alpha^{+/+}$  sham group). Two weeks after OVX, the bone phenotype was analyzed.

(B) BMD of the distal femurs within each group are described in Figure 3A (\* $p < 0.05$ ; N.S., not significant). Data are represented as mean  $\pm$  SEM.

(C) Cortical thickness evaluation from micro CT analysis of femurs within each group described in Figure 3A. Data are represented as mean  $\pm$  SEM.

(D) The levels of  $TNF\alpha$ ,  $IL-1\alpha$ , and  $IL-6$  in the bone-marrow cells culture media and serum RANKL (\* $p < 0.05$  compared to each sham group). Data are represented as mean  $\pm$  SEM.

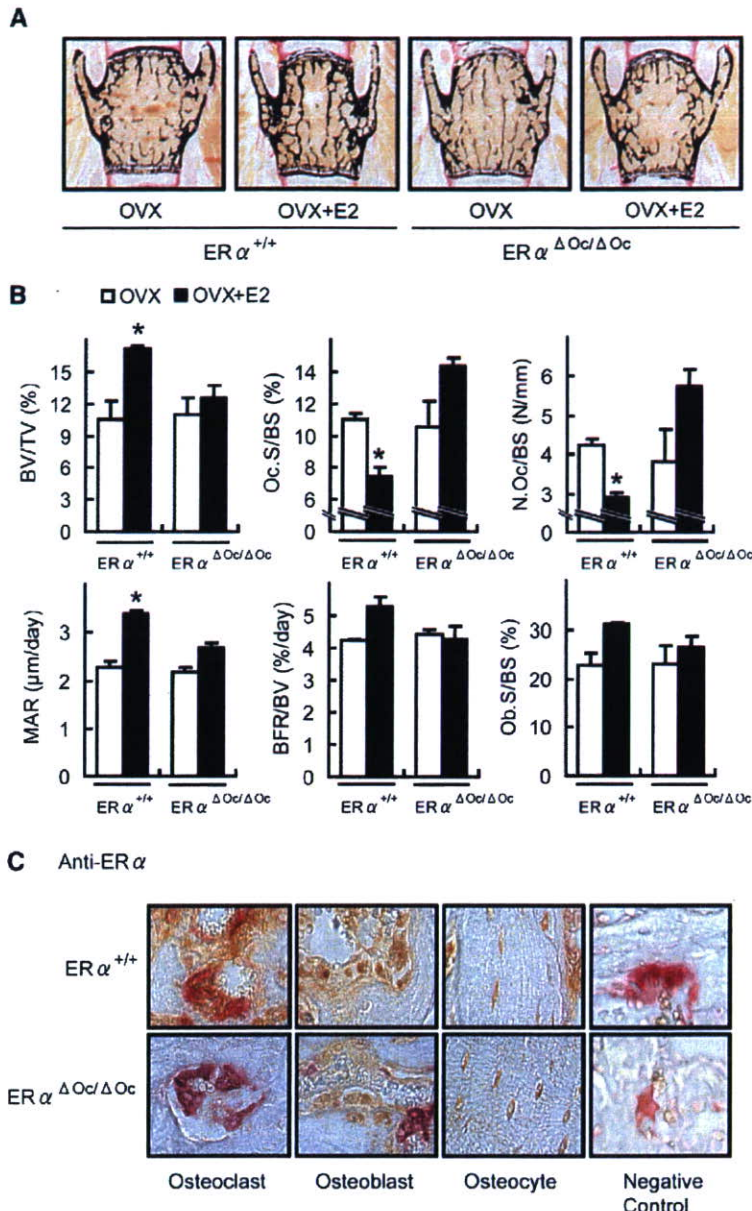


**Figure 4. Estrogen treatment failed to reverse trabecular bone loss of ovariectomized  $ER\alpha^{\Delta Ocl/\Delta Ocl}$  females**

(A) von kossa staining of lumbar vertebral bodies of ovariectomized  $ER\alpha^{+/+}$  and  $ER\alpha^{\Delta Ocl/\Delta Ocl}$  mice treated with or without 17 $\beta$ -estradiol (0.83  $\mu\text{g}/\text{day}$ ) for 2 weeks (+E2) groups.

(B) Bone histomorphometrical analyses of the lumbar vertebral bodies of 12-week-old ovariectomized  $ER\alpha^{+/+}$  (left columns) and  $ER\alpha^{\Delta Ocl/\Delta Ocl}$  (right columns) mice with (filled columns) or without (open columns) E2 treatment for 2 weeks (\* $p < 0.05$  compared with E2-treated ovariectomized  $ER\alpha^{\Delta Ocl/\Delta Ocl}$  mice). BV/TV: bone volume per tissue volume. ES/BS: eroded surface per bone surface. Oc.S/BS: osteoclast surface per bone surface. N.Oc/BS: osteoclast number per bone surface. MS/BS: mineralizing surface per bone surface. Ob.S/BS: osteoblast surface per bone surface. MAR: mineral apposition rate. BFR/BS: bone formation rate per bone surface. Data are represented as mean  $\pm$  SEM.

(C) Immunohistochemical identification of  $ER\alpha$  (brown) in TRAP-positive (red) differentiated osteoclasts. The femurs of 12 week-old mice were used for the immunodetection of  $ER\alpha$  in bone cells. All labels were abolished when the primary antibody was preadsorbed with the immunizing peptide (negative control).

The number of TRAP-positive osteoclasts differentiated from the bone-marrow cells of  $ER\alpha^{\Delta Ocl/\Delta Ocl}$  females was almost the same as that from  $ER\alpha^{+/+}$  females (Figure 5A) and males (data not shown). The differentiated  $ER\alpha^{\Delta Ocl/\Delta Ocl}$  osteoclasts had typical osteoclastic features, including the characteristic cell shape, TRAP-positive, multiple nuclei, and actin-ring formation, and were indistinguishable from the  $ER\alpha^{+/+}$  osteoclasts (Figure 5B).

The expression levels of the prime osteoclastogenic transcription factors, *c-fos* and *NFATc1*, were unaltered by  $ER\alpha$  deficiency in differentiated osteoclasts (Figure 5C). Furthermore, responses to RANKL in intracellular signaling, as represented by phosphorylation of p38

and I $\kappa$ B, were unaffected in  $ER\alpha^{\Delta Ocl/\Delta Ocl}$  osteoclasts from females (Figure 5D) as well as males (data not shown). In light of these findings, it is unlikely that activated  $ER\alpha$  in osteoclastic cells attenuates osteoclastogenesis.

#### Activation of the Fas/FasL System by Estrogen in Intact Bone Is Impaired by Osteoclastic $ER\alpha$ Deficiency

To examine osteoclastic  $ER\alpha$  function in intact bone, DNA microarray analysis following real-time RT-PCR of RNA from the femurs of ovariectomized  $ER\alpha^{\Delta Ocl/\Delta Ocl}$  females treated with or without estrogen, was performed. During

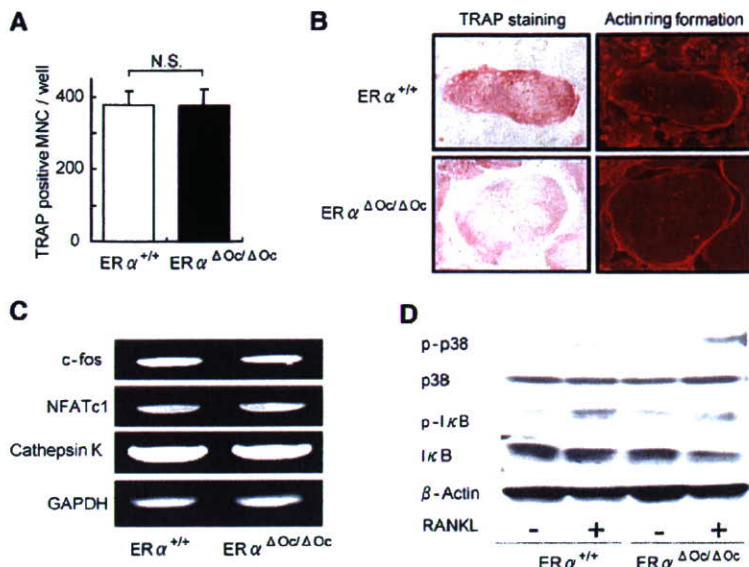


**Figure 5. ER $\alpha$  Deficiency Did Not Affect Osteoclastogenesis**

(A) TRAP-positive multinucleated cell count at 3 days after RANKL stimulation, cultured in 24-well plates ( $n = 6$ , N.S., not significant). Data are represented as mean  $\pm$  SEM.

(B) TRAP staining and actin ring formation of RANKL induced primary cultured osteoclasts from bone-marrow cells of ER $\alpha^{+/+}$  and ER $\alpha^{\Delta Oc/\Delta Oc}$  mice.

(C) RT-PCR analysis of genes related to osteoclastogenesis.

(D) Western blot analysis of phosphorylated p38, JNK, and I $\kappa$ B of primary cultured bone-marrow cells stimulated with or without 100 ng/ml of RANKL for 15 min.

the search for candidate ER $\alpha$  target genes in bone by DNA microarray analysis (Figure S3), we found that a number of apoptosis-related factors were regulated by estrogen in the intact bone of ER $\alpha^{+/+}$  females but dysregulated in ER $\alpha^{\Delta Oc/\Delta Oc}$  females. This observation is consistent with a previous report of estrogen-induced apoptosis of mature osteoclasts (Kameda et al., 1997). Real-time RT-PCR to validate the estrogen regulations of the candidate genes revealed that gene expression of *FasL*, an apoptotic factor, was responsive to E2 (Figure 6A). Estrogen treatment (+E2) indeed induced expression of FasL protein in bone of ovariectomized ER $\alpha^{+/+}$ , but this induction was not obvious in ovariectomized ER $\alpha^{\Delta Oc/\Delta Oc}$  mice (Figures 6B and 6C). Reflecting FasL induction by estrogen, estrogen-induced apoptosis (as observed by the TUNEL assay) in TRAP-positive mature trabecular osteoclasts in the distal femurs of the ER $\alpha^{+/+}$  mice was detected, but this E2 response was abolished in the ER $\alpha^{\Delta Oc/\Delta Oc}$  mice (Figure 6D). Furthermore, in mice lacking functional FasL (*FasL<sup>gld/gld</sup>*), neither enhanced bone resorption nor bone mass loss was induced by ovariectomy (Figures 6E and 6F).

#### Osteoclastic ER $\alpha$ Mediates Estrogen-Induced apoptosis by FasL

The expression level of ER $\alpha$  protein in differentiated osteoclasts derived from bone marrow cells was very low, but induction of *FasL* gene expression was also detectable in the cultured osteoclasts of ER $\alpha^{+/+}$  females as well as males (Figure 7A). However, this E2 response was impaired in cultured osteoclasts from ER $\alpha^{\Delta Oc/\Delta Oc}$  females (Figure 7A). It is notable that such responses are also induced by tamoxifen (Figure 7C), which is an osteoprotective SERM (Harada and Rodan, 2003). ER $\alpha$  overexpression augmented *FasL* gene expression in response to estrogen in cultured osteoclasts from ER $\alpha^{\Delta Oc/\Delta Oc}$  females

(Figure S4A). In primary cultured calvarial osteoblasts from females as well as males (Suzawa et al., 2003), *FasL* gene induction by E2 and tamoxifen was also seen; however, it was not accompanied by increased apoptosis (data not shown). Thus, it appears that estrogen-induced apoptosis in osteoclasts is mediated by FasL expression in osteoclasts in the trabecular bone areas, presumably as well as in osteoblasts in cortical bone areas. As expected, the cell number of TUNEL-positive osteoclasts was increased by E2 in the cultured osteoclasts from ER $\alpha^{+/+}$  females, but E2-induced apoptosis was undetectable in ER $\alpha^{\Delta Oc/\Delta Oc}$  osteoclasts (Figure 7B). Consistent with FasL-induced apoptosis, *Fas* gene expression was observed (Figure 7D), but it was likely that Fas expression did not require ER $\alpha$  function (Figures S4B and S4C). Expression levels of *Fas* and ER $\alpha$  as well as E2 response in apoptosis appeared to fluctuate during osteoclast differentiation (Figures S4B–S4D); however, in FasL mutant (*FasL<sup>gld/gld</sup>*) females, the E2-induced apoptosis was abolished (Figure S4E). These findings suggest that activated ER $\alpha$  in differentiated osteoclasts induces apoptosis through activating FasL/Fas signaling. This leads to suppression of bone resorption through truncating the already short life span of differentiated osteoclasts (Teitelbaum, 2006).

#### DISCUSSION

Selective ablation of ER $\alpha$  in mature osteoclasts in female mice shows that the osteoprotective effect of estrogen is mediated by osteoclastic ER $\alpha$ , at least in the trabecular regions of the tibiae, femur, and lumbar vertebrae of female mice. Activated ER $\alpha$  by estrogen as well as SERMs appears to truncate the already short life span (estimated at 2 weeks) of differentiated osteoclasts by inducing apoptosis through activation of the Fas/FasL system.

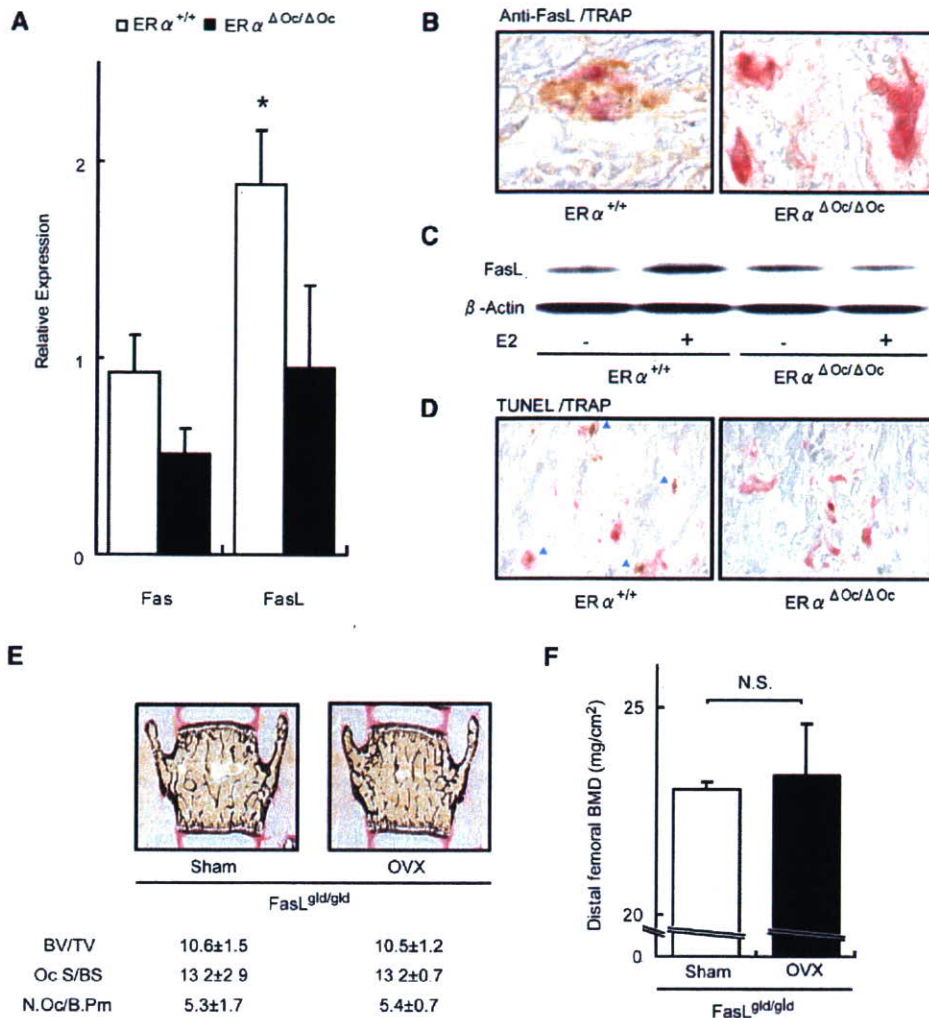


**Figure 6. Activated  $ER\alpha$  Induced Fas Ligand Expression and Apoptosis in Differentiated Osteoclasts of Intact Bone**

(A) Real-time RT-PCR analysis of *Fas* and *FasL*. Expression levels in bones from E2-treated ovariectomized  $ER\alpha^{+/+}$  (open column) and  $ER\alpha^{\Delta Oc/\Delta Oc}$  (filled column) were compared with the ovariectomized groups of each genotype without E2 administration ( $*p < 0.05$  compared to  $ER\alpha^{+/+}$ ). Data are represented as mean  $\pm$  SEM.

(B) Immunohistochemical analysis of anti-FasL with TRAP staining of the sections from the distal femurs of E2-treated ovariectomized  $ER\alpha^{+/+}$  and  $ER\alpha^{\Delta Oc/\Delta Oc}$  mice. Brown stained cells are anti-FasL positive.

(C) Anti-FasL western blot analysis of proteins obtained from femurs of ovariectomized  $ER\alpha^{+/+}$  and  $ER\alpha^{\Delta Oc/\Delta Oc}$  mice treated with or without E2, using anti- $\beta$ -actin as internal control.

(D) TUNEL staining with TRAP staining of the sections from the distal femurs of E2-treated ovariectomized  $ER\alpha^{+/+}$  and  $ER\alpha^{\Delta Oc/\Delta Oc}$  mice. Arrowheads indicate both TUNEL (brown)- and TRAP-positive staining cells.

(E) Bone histomorphometrical analysis of sham-operated or ovariectomized  $FasL^{gld/gld}$  mice.

(F) BMD of the distal femurs of sham operated or ovariectomized  $FasL^{gld/gld}$  mice. Data are represented as mean  $\pm$  SEM.

This attenuates bone resorption. This idea is supported by previous observations that estrogen deficiency following menopause or ovariectomy leads to high bone turnover, particularly in the trabecular areas, as bone is rapidly lost through enhanced resorption (Delmas, 2002; Tolar et al., 2004). Thus, estrogen treatment leads to recovery from osteopenia by reducing resorption (Delmas, 2002; Rodan and Martin, 2000), partly by the induction of osteoclast cell death.

In contrast to the osteopenia seen in the  $ER\alpha^{\Delta Oc/\Delta Oc}$  females, the  $ER\alpha^{\Delta Oc/\Delta Oc}$  male mice unexpectedly had no bone loss. The male mice still demonstrated an  $ER\alpha$ -mediated induction of FasL in response to estrogen with subsequent apoptosis of osteoclasts (Figure 7). Both male mice with a deficiency of aromatase that are unable to locally produce estrogen from testosterone and men with a genetic mutation in the  $ER\alpha$  gene suffer from osteoporosis (Smith et al., 1994). Considering that the

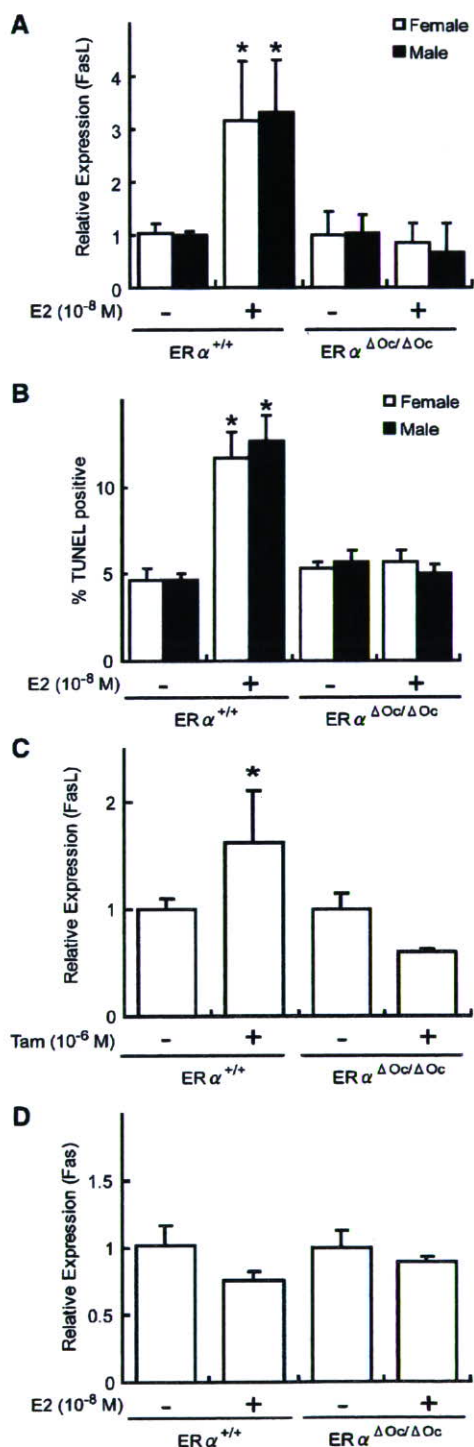


**Figure 7. Estrogen-Induced *FasL* Expression and Apoptosis Required ER $\alpha$  in Cultured Osteoclasts**

(A) Real-time RT-PCR analysis of *FasL* expression using total RNA obtained from in vitro primary cultured osteoclasts of each genotype at 3 days after RANKL stimulation, treated with or without E2 (10<sup>-8</sup> M) for 4 hr (\**p* < 0.05 compared to the group treated without E2). Data are represented as mean  $\pm$  SEM.

markedly elevated levels of testosterone in ER $\alpha$  KO females may be potent enough to maintain normal bone turnover (Syed and Khosla, 2005), it is likely that the activated AR might be functionally sufficient in male mice to compensate for the ER $\alpha$  deficiency in bone (Kawano et al., 2003). However, species differences in the osteoprotective action of sex steroid hormones still need to be carefully addressed.

Fas/FasL system-mediated apoptotic induction of osteoclasts by estrogen may well be a part of the mechanism for the antiresorptive action of estrogen and SERMs in trabecular bone areas (Delmas, 2002; Rodan and Martin, 2000; Simpson and Davis, 2001; Syed and Khosla, 2005; Tolar et al., 2004). Regulation of osteoclast differentiation is tightly coupled to osteoblastic function in terms of cytokine production and cell-cell contact (Karsenty and Wagner, 2002; Martin and Sims, 2005; Mundy and Elefteriou, 2006; Teitelbaum and Ross, 2003). Indeed, upregulation of osteoclastogenic cytokines by ovariectomy was unaffected in ER $\alpha$ <sup>ΔOc/ΔOc</sup> females. Considering the observation that cortical bone mass is increased in ovariectomized ER $\alpha$ <sup>ΔOc/ΔOc</sup> females during estrogen treatment, it is conceivable that the antiresorptive estrogen action in cortical bone is also mediated by osteoblastic ER $\alpha$ . In this regard, FasL induction by estrogen in osteoblasts may contribute to the osteoprotective estrogen action, and *FasL* gene induction by estrogen was in fact detected in primary cultured osteoblasts from female calvaria by us as well as another group (S. Krum and M. Brown, personal communication). Thus, similar experiments in which ER $\alpha$  is selectively ablated in osteoblasts are needed to define the role of ER $\alpha$  in these cells.

In osteoclastic cells, expression of the *FasL* gene, which leads to apoptosis, appears to be positive controlled by activated ER $\alpha$ . Not surprisingly, a direct binding site for ER $\alpha$  has been mapped in the *FasL* gene locus (S. Krum and M. Brown, personal communication). An osteoclast- and cell-differentiation stage-specific mechanism may underlie this gene induction in the *FasL* gene promoter. A recent study demonstrated that ER $\alpha$  recruitment to specific promoter sites of given ER $\alpha$  target genes was cell-type specific (Carroll et al., 2005). Thus, there is significant impetus to identify the osteoclastic factor that associates with ER $\alpha$  in the *FasL* gene promoter. Such identification will lead to a better understanding of the molecular basis of the osteoprotective estrogen action and provide a target against which to develop SERMs of greater effectiveness.

(B) Apoptotic cells were defined as those with TUNEL-positive nuclei among TRAP-positive multinucleated primary cultured osteoclasts treated with or without E2 (10<sup>-8</sup> M) for 12 hr in 96-well plates (\**p* < 0.05 compared to the group treated without E2). Data are represented as mean  $\pm$  SEM.

(C) *FasL* expression in each genotypic female osteoclastic cells treated with or without Tam (10<sup>-6</sup> M) (\**p* < 0.05 compared to the group treated without Tam). Data are represented as mean  $\pm$  SEM.

(D) Expression of *Fas* was measured as described in the legend of Figure 7A. Data are represented as mean  $\pm$  SEM.

## EXPERIMENTAL PROCEDURES

### *Ctsk*-Cre Construction and Generation of the Knockin Mouse Lines

An RP23-422n18 BAC clone containing the mouse *Ctsk* gene was purchased from Invitrogen (Carlsbad, CA). The *FRT-Kar<sup>f</sup>/Neo<sup>f</sup>-FRT* and *nlsCre* fragments were obtained from plasmids pSK2/3-*FRT-Neo* and pC-Cre. Two homologous arms of 500 bp from the *Ctsk* gene were inserted into both sides of the *nlsCre-FRT-Kar<sup>f</sup>/Neo<sup>f</sup>-FRT* cassette in the pSK2/3-*FRT-Neo* plasmid. The *nlsCre-FRT-Kar<sup>f</sup>/Neo<sup>f</sup>-FRT* cassette was introduced into the endogenous ATG start site of the *Ctsk* gene by recombineering approaches (Copeland et al., 2001). Targeted BAC was reduced in size from 189 kb to 26 kb and subcloned into the pMC1-DTPA vector by the gap-repair method. The targeted T2 ES clones were selected after positive-negative selection with G418 and DT-A with Southern analysis, then aggregated with single eight-cell embryos from CD-1 mice (Yoshizawa et al., 1997). Chimeric mice were then crossed with a general deleter mouse line, *ACTB-Fipe* (Jackson Laboratory), to remove the *Kar<sup>f</sup>/Neo<sup>f</sup>* cassette. The *Ctsk-Cre* mice (*Ctsk<sup>Cre/+</sup>*), originally on a hybrid C57BL/6 and CBA genetic background, were backcrossed for four generations into a C57BL/6J background. *FasL<sup>gld/gld</sup>* mice were also purchased from Jackson Laboratory.

### Analysis of Cre Recombinase Activities

Expression of the Cre transcript was detected by RT-PCR. Southern analysis using a Cre cDNA probe was performed with total RNA extracted from 12-week-old mice. To evaluate the specificity and efficiency of Cre-mediated recombination, we mated the *Ctsk<sup>Cre/+</sup>* mice to CAG-CAT-Z reporter mice (kindly provided by J. Miyazaki) (Sakai and Miyazaki, 1997) and genotyped their offspring with Cre-specific primers.  $\beta$ -galactosidase activity of the expressed LacZ gene driven by the CAG promoter was expected to be detected in the given cells expressing functional Cre recombinase.

### In Vitro Osteoclastogenesis and Ligand Application

Bone-marrow cells derived from 8-week-old mice were plated in culture dishes containing  $\alpha$ -MEM (GIBCO-BRL) with 10% FBS (JRH) and 10 ng/ml M-CSF (Genzyme). After incubation for 48 hr, adherent cells were used as osteoclast precursor cells after washing out the nonadherent cells. Cells were cultured in the presence of 10 ng/ml M-CSF and 100 ng/ml RANKL (Peprotech) to generate osteoclast-like cells (Koga et al., 2004) for 3 days, so the total culture time was 5 days. Three days after RANKL stimulation, primary cultured osteoclasts were treated with  $10^{-8}$  M of 17 $\beta$ -estradiol (E2) (Sigma-Aldrich Co.) or  $10^{-6}$  M 4-hydroxytamoxifen (Tam) (Sigma-Aldrich Co.) in phenol-red free medium.

### Generation of Osteoclast-Specific ER $\alpha$ KO Mice

The ER $\alpha$  conditional (*ER $\alpha$ <sup>flax/flax</sup>*) (Dupont et al., 2000) and null alleles with a C57BL/6J background have been previously described. *ER $\alpha$ <sup>flax/flax</sup>* mice were crossed with *Ctsk<sup>Cre/+</sup>* mice to generate *Ctsk<sup>Cre/+</sup>; ER $\alpha$ <sup>flax/+</sup>* mice. *Ctsk<sup>Cre/+</sup>; ER $\alpha$ <sup>+/+</sup>* (*ER $\alpha$ <sup>+/+</sup>*) and *Ctsk<sup>Cre/+</sup>; ER $\alpha$ <sup>flax/flax</sup>* (*ER $\alpha$ <sup>ΔOcl/ΔOcl</sup>*) mice were obtained by crossing *Ctsk<sup>Cre/+</sup>; ER $\alpha$ <sup>flax/+</sup>* with *ER $\alpha$ <sup>flax/+</sup>* mouse lines.

### Radiological Analysis

Bone radiographs of the femurs of 12-week-old *Ctsk<sup>Cre/+</sup>; ER $\alpha$ <sup>flax/flax</sup>* (*ER $\alpha$ <sup>ΔOcl/ΔOcl</sup>*) and *Ctsk<sup>Cre/+</sup>; ER $\alpha$ <sup>+/+</sup>* (*ER $\alpha$ <sup>+/+</sup>*) littermates were visualized with a soft X-ray apparatus (TRS-1005; SOFTRON). BMD was measured by DXA using a bone mineral analyzer (DCS-600EX; ALOKA). Micro Computed Tomography scanning of the femurs was performed using a composite X-ray analyzer (NX-CP-C80H-IL; Nit-tetsu ELEX Co.) (Kawano et al., 2003). Tomograms were obtained with a slice thickness of 10  $\mu$ m and reconstructed at 12  $\times$  12 pixels into a 3D image by the volume-rendering method (VIP-Station; Teijin System Technology) using a computer.

### Analysis of Skeletal Morphology

Twelve-week-old *Ctsk<sup>Cre/+</sup>; ER $\alpha$ <sup>flax/flax</sup>* (*ER $\alpha$ <sup>ΔOcl/ΔOcl</sup>*) and *Ctsk<sup>Cre/+</sup>; ER $\alpha$ <sup>+/+</sup>* (*ER $\alpha$ <sup>+/+</sup>*) littermates were double labeled with subcutaneous injections of 16 mg/kg of calcein (Sigma) at 4 and 2 days before sacrifice. Tibiae were removed from each mouse and fixed with 70% ethanol. They were stained with Villanueva bone stain for 7 days and embedded in methyl-methacrylate (Wako) (Yoshizawa et al., 1997). Frontal plane sections (5- $\mu$ m thick) of the proximal tibia were cut using a Microtome (LEICA). The cancellous bone was measured in the secondary spongiosa located 500  $\mu$ m from the epiphyseal growth plate and 160  $\mu$ m from the endocortical surface (Kawano et al., 2003; Nakamichi et al., 2003). Bone histomorphometric measurements of the tibia were made using a semiautomatic image analyzing system (System Supply) and a fluorescent microscope (Optiphot; Nikon). Similar measurements of the lumbar vertebral bodies were done as previously reported (Takeda et al., 2002). Standard bone histomorphometrical nomenclatures, symbols, and units were used as described in the report of the ASBMR Histomorphometry Nomenclature Committee.

### Ovariectomy and Hormone Replacement

Female *Ctsk<sup>Cre/+</sup>; ER $\alpha$ <sup>flax/flax</sup>* (*ER $\alpha$ <sup>ΔOcl/ΔOcl</sup>*) and *Ctsk<sup>Cre/+</sup>; ER $\alpha$ <sup>+/+</sup>* (*ER $\alpha$ <sup>+/+</sup>*) littermates were ovariectomized or sham operated at 8–12 weeks of age for 2 weeks for all experiments, and slow releasing pellets of E2 (0.83  $\mu$ g/day) or placebo (Innovative Research, Sarasota, FL) were implanted subcutaneously in the scapular region behind the neck (Sato et al., 2004; Shiina et al., 2006).

### Immunohistochemistry

Twelve-week-old *Ctsk<sup>Cre/+</sup>; ER $\alpha$ <sup>flax/flax</sup>* (*ER $\alpha$ <sup>ΔOcl/ΔOcl</sup>*) and *Ctsk<sup>Cre/+</sup>; ER $\alpha$ <sup>+/+</sup>* (*ER $\alpha$ <sup>+/+</sup>*) littermates were fixed with 4% PFA by perfusion. Serial sections of the brain (20  $\mu$ m thick) were divided into two groups and used for single labeling for the ER $\alpha$  or thionin to allow determination of the areas to be measured. Tibiae and femurs were decalcified in 10% EDTA for 2–4 weeks after fixation and then embedded in paraffin sections. Sections were incubated in L.A.B. solution (Polysciences) for 30 min to retrieve antigen. The cooled sections were incubated in 1% H<sub>2</sub>O<sub>2</sub> for 30 min to quench endogenous peroxidase and then washed with 1% Triton X-100 in PBS for 10 min. To block nonspecific antibody binding, sections were incubated in blocking solution (DAKO) for 5 min. Sections were then incubated with anti-ER $\alpha$  (Santa Cruz, CA) and anti-FasL (Santa Cruz, CA) in blocking solution overnight at 4°C. Staining was then performed using the EnVision+ HRP System (Dako) and 3, 3'-diaminobenzidine tetrahydrochloride substrate (Sigma), counterstained with TRAP, dehydrated through an ethanol series and xylene, before mounting (Sato et al., 2004).

### ER $\alpha$ Overexpression

Two days after RANKL stimulation, an expression vector of mouse ER $\alpha$  was transfected into immature osteoclastic cells from *ER $\alpha$ <sup>ΔOcl/ΔOcl</sup>* mice using Superfect (QIAGEN) as manufacture's instruction.

### Real-Time RT-PCR

One microgram of total RNA from each sample was reverse transcribed into first-strand cDNA with random hexamers using Super-script III reverse transcriptase (Invitrogen). Primer sets for all genes were purchased from Takara Bio. Inc. (Tokyo, Japan). Real-time RT-PCR was performed using SYBR Premix Ex Taq (Takara) with the ABI PRISM 7900HT (Applied Biosystems) according to the manufacturer's instructions. Experimental samples were matched to a standard curve generated by amplifying serially diluted products using the same PCR protocol. To correct for variability in RNA recovery and efficiency of reverse transcription, *Gapdh* cDNA was amplified and quantified in each cDNA preparation. Normalization and calculation steps were performed as reported previously (Takezawa et al., 2007).

### TUNEL/TRAP Staining

The TUNEL method was performed using the ApopTag Fluorescein In Situ Apoptosis Detection Kit (CHEMICON international) according to the manufacturer's instructions with a slight modification. This was followed by TRAP staining as previously reported (Kobayashi et al., 2000).

### Cytokine Assays

Bone marrow and blood were collected at 2 weeks after sham operation or ovariectomy. Bone-marrow cells were cultured for 3 days in DMEM. The levels of TNF $\alpha$ , IL-1 $\alpha$ , and IL-6 in the culture media and serum RANKL were determined by ELISA (R&D Systems).

### Western Blot

Osteoclast precursor cells were treated with or without 100 ng/ml of soluble RANKL. After 15 minutes, cell extracts were harvested from the cells using lysis buffer containing 100 mM Tris-HCl (pH 7.8), 150 mM NaCl, 0.1% Triton X-100, 5% protease inhibitor cocktail (Sigma), and 5% phosphatase inhibitor cocktail (Sigma). An equivalent amount of protein from each of the cell extracts and proteins of femoral bone extracted using ISOGEN was loaded for SDS-PAGE and transferred to PVDF membranes (Amersham Biosciences). The membranes were developed with enhanced chemiluminescence reagent (Amersham Biosciences) (Ohtake et al., 2003). Phosphorylation of p38 MAPK and I $\kappa$ B were evaluated using antibodies purchased from Cell Signaling Technology (Koga et al., 2004) and anti-FasL antibody was purchased from Santa Cruz Biotechnology (sc-834).

### Actin-Ring Formation

Cells were fixed for 15 min in warm 4% paraformaldehyde (PFA). After fixation, cells were washed three times with PBS with 0.1% Triton X-100 (PBST) and incubated with 0.2 U/ml rhodamine phalloidin (Molecular Probes) for 30 min and washed again three times in PBST.

### Statistical Analysis

Data were analyzed by two-tailed student's *t* test. For all graphs, data are represented as mean  $\pm$  SEM.

### Supplemental Data

Supplemental Data include Supplemental Experimental Procedures and four figures and can be found with this article online at <http://www.cell.com/cgi/content/full/130/5/811/DC1/>.

### ACKNOWLEDGMENTS

We thank Drs. S. Krum and M. Brown to share with their unpublished results; Drs. K. Yoshimura, Y. Nakamichi, T. Watanabe, J. Miyamoto, H. Shiina, T. Fukuda, Ms. Y. Sato, and S. Tanaka for generation of the KO mice; Drs. T. Koga, H. Takagi, E. Ochiai, and N. Moriyama for technical help; Dr. J. Miyazaki for CAG-CAT-Z reporter mice, and H. Higuchi and K. Hiraga for manuscript preparation. This work was supported in part by priority areas from the Ministry of Education, Culture, Sports, Science and Technology (to S.K.) and the Program for Promotion of Basic Research Activities for Innovative Biosciences (PROBRAIN).

Received: February 23, 2007

Revised: May 21, 2007

Accepted: July 17, 2007

Published: September 6, 2007

### REFERENCES

Belandia, B., and Parker, M.G. (2003). Nuclear receptors: a rendezvous for chromatin remodeling factors. *Cell* 114, 277–280.

Bland, R. (2000). Steroid hormone receptor expression and action in bone. *Clin. Sci. (Lond.)* 98, 217–240.

Carroll, J.S., Liu, X.S., Brodsky, A.S., Li, W., Meyer, C.A., Szary, A.J., Eeckhoutte, J., Shao, W., Hestermann, E.V., Geistlinger, T.R., et al. (2005). Chromosome-wide mapping of estrogen receptor binding reveals long-range regulation requiring the forkhead protein FoxA1. *Cell* 122, 33–43.

Chien, K.R., and Karsenty, G. (2005). Longevity and lineages: toward the integrative biology of degenerative diseases in heart, muscle, and bone. *Cell* 120, 533–544.

Copeland, N.G., Jenkins, N.A., and Court, D.L. (2001). Recombineering: a powerful new tool for mouse functional genomics. *Nat. Rev. Genet.* 2, 769–779.

Couse, J.F., and Korach, K.S. (1999). Estrogen receptor null mice: what have we learned and where will they lead us? *Endocr. Rev.* 20, 358–417.

Delmas, P.D. (2002). Treatment of postmenopausal osteoporosis. *Lancet* 359, 2018–2026.

Dupont, S., Krust, A., Gansmuller, A., Dierich, A., Chambon, P., and Mark, M. (2000). Effect of single and compound knockouts of estrogen receptors alpha (ERalpha) and beta (ERbeta) on mouse reproductive phenotypes. *Development* 127, 4277–4291.

Gowen, M., Lazner, F., Dodds, R., Kapadia, R., Feild, J., Tavaría, M., Bertoncello, I., Drake, F., Zavarselk, S., Tellis, I., et al. (1999). Cathepsin K knockout mice develop osteopetrosis due to a deficit in matrix degradation but not demineralization. *J. Bone Miner. Res.* 14, 1654–1663.

Harada, S., and Rodan, G.A. (2003). Control of osteoblast function and regulation of bone mass. *Nature* 423, 349–355.

Kameda, T., Mano, H., Yuasa, T., Mori, Y., Miyazawa, K., Shiokawa, M., Nakamaru, Y., Hiroi, E., Hiura, K., Kameda, A., et al. (1997). Estrogen inhibits bone resorption by directly inducing apoptosis of the bone-resorbing osteoclasts. *J. Exp. Med.* 186, 489–495.

Karsenty, G. (2006). Convergence between bone and energy homeostases: leptin regulation of bone mass. *Cell Metab.* 4, 341–348.

Karsenty, G., and Wagner, E.F. (2002). Reaching a genetic and molecular understanding of skeletal development. *Dev. Cell* 2, 389–406.

Kato, S., Ito, S., Noguchi, T., and Naito, H. (1989). Effects of brefeldin A on the synthesis and secretion of egg white proteins in primary cultured oviduct cells of laying Japanese quail (*Coturnix coturnix japonica*). *Biochim. Biophys. Acta* 991, 36–43.

Kawano, H., Sato, T., Yamada, T., Matsumoto, T., Sekine, K., Watanabe, T., Nakamura, T., Fukuda, T., Yoshimura, K., Yoshizawa, T., et al. (2003). Suppressive function of androgen receptor in bone resorption. *Proc. Natl. Acad. Sci. USA* 100, 9416–9421.

Kimble, R.B., Matayoshi, A.B., Vannice, J.L., Kung, V.T., Williams, C., and Pacifici, R. (1995). Simultaneous block of interleukin-1 and tumor necrosis factor is required to completely prevent bone loss in the early postovariectomy period. *Endocrinology* 136, 3054–3061.

Kobayashi, Y., Hashimoto, F., Miyamoto, H., Kanaoka, K., Miyazaki-Kawashita, Y., Nakashima, T., Shibata, M., Kobayashi, K., Kato, Y., and Sakai, H. (2000). Force-induced osteoclast apoptosis in vivo is accompanied by elevation in transforming growth factor beta and osteoprotegerin expression. *J. Bone Miner. Res.* 15, 1924–1934.

Koga, T., Inui, M., Inoue, K., Kim, S., Suematsu, A., Kobayashi, E., Iwata, T., Ohnishi, H., Matozaki, T., Kodama, T., et al. (2004). Costimulatory signals mediated by the ITAM motif cooperate with RANKL for bone homeostasis. *Nature* 428, 758–763.

Li, C.Y., Jepsen, K.J., Majeska, R.J., Zhang, J., Ni, R., Gelb, B.D., and Schaffler, M.B. (2006). Mice lacking Cathepsin K maintain bone remodeling but develop bone fragility despite high bone mass. *J. Bone Miner. Res.* 21, 865–875.

- Mangelsdorf, D.J., Thummel, C., Beato, M., Herrlich, P., Schutz, G., Umesono, K., Blumberg, B., Kastner, P., Mark, M., Chambon, P., and Evans, R.M. (1995). The nuclear receptor superfamily: the second decade. *Cell* 83, 835–839.
- Martin, T.J., and Sims, N.A. (2005). Osteoclast-derived activity in the coupling of bone formation to resorption. *Trends Mol. Med.* 11, 76–81.
- Mueller, S.O., and Korach, K.S. (2001). Estrogen receptors and endocrine diseases: lessons from estrogen receptor knockout mice. *Curr. Opin. Pharmacol.* 1, 613–619.
- Mundy, G.R., and Eleftheriou, F. (2006). Boning up on ephrin signaling. *Cell* 126, 441–443.
- Nakamichi, Y., Shukunami, C., Yamada, T., Aihara, K., Kawano, H., Sato, T., Nishizaki, Y., Yamamoto, Y., Shindo, M., Yoshimura, K., et al. (2003). Chondromodulin I is a bone remodeling factor. *Mol. Cell. Biol.* 23, 636–644.
- Ohtake, F., Takeyama, K., Matsumoto, T., Kitagawa, H., Yamamoto, Y., Nohara, K., Tohyama, C., Krust, A., Mimura, J., Chambon, P., et al. (2003). Modulation of oestrogen receptor signalling by association with the activated dioxin receptor. *Nature* 423, 545–550.
- Raisz, L.G. (2005). Pathogenesis of osteoporosis: concepts, conflicts, and prospects. *J. Clin. Invest.* 115, 3318–3325.
- Riggs, B.L., and Hartmann, L.C. (2003). Selective estrogen-receptor modulators—mechanisms of action and application to clinical practice. *N. Engl. J. Med.* 348, 618–629.
- Rodan, G.A., and Martin, T.J. (2000). Therapeutic approaches to bone diseases. *Science* 289, 1508–1514.
- Saftig, P., Hunziker, E., Wehmeyer, O., Jones, S., Boyde, A., Rommerskirch, W., Moritz, J.D., Schu, P., and von Figura, K. (1998). Impaired osteoclastic bone resorption leads to osteopetrosis in Cathepsin-K-deficient mice. *Proc. Natl. Acad. Sci. USA* 95, 13453–13458.
- Sakai, K., and Miyazaki, J. (1997). A transgenic mouse line that retains Cre recombinase activity in mature oocytes irrespective of the cre transgene transmission. *Biochem. Biophys. Res. Commun.* 237, 318–324.
- Sato, T., Matsumoto, T., Kawano, H., Watanabe, T., Uematsu, Y., Sekine, K., Fukuda, T., Aihara, K., Krust, A., Yamada, T., et al. (2004). Brain masculinization requires androgen receptor function. *Proc. Natl. Acad. Sci. USA* 101, 1673–1678.
- Shang, Y., and Brown, M. (2002). Molecular determinants for the tissue specificity of SERMs. *Science* 295, 2465–2468.
- Shiina, H., Matsumoto, T., Sato, T., Igarashi, K., Miyamoto, J., Takemasa, S., Sakari, M., Takada, I., Nakamura, T., Metzger, D., et al. (2006). Premature ovarian failure in androgen receptor-deficient mice. *Proc. Natl. Acad. Sci. USA* 103, 224–229.
- Simpson, E.R., and Davis, S.R. (2001). Minireview: aromatase and the regulation of estrogen biosynthesis—some new perspectives. *Endocrinology* 142, 4589–4594.
- Sims, N.A., Clement-Lacroix, P., Minet, D., Fraslon-Vanhulle, C., Gaillard-Kelly, M., Resche-Rigon, M., and Baron, R. (2003). A functional androgen receptor is not sufficient to allow estradiol to protect bone after gonadectomy in estradiol receptor-deficient mice. *J. Clin. Invest.* 111, 1319–1327.
- Smith, E.P., Boyd, J., Frank, G.R., Takahashi, H., Cohen, R.M., Specker, B., Williams, T.C., Lubahn, D.B., and Korach, K.S. (1994). Estrogen resistance caused by a mutation in the estrogen-receptor gene in a man. *N. Engl. J. Med.* 331, 1056–1061.
- Sun, L., Peng, Y., Sharrow, A.C., Iqbal, J., Zhang, Z., Papachristou, D.J., Zaidi, S., Zhu, L.L., Yaroslavskiy, B.B., Zhou, H., et al. (2006). FSH directly regulates bone mass. *Cell* 125, 247–260.
- Suzawa, M., Takada, I., Yanagisawa, J., Ohtake, F., Ogawa, S., Yamauchi, T., Kadowaki, T., Takeuchi, Y., Shibuya, H., Gotoh, Y., et al. (2003). Cytokines suppress adipogenesis and PPAR-gamma function through the TAK1/TAB1/NIK cascade. *Nat. Cell Biol.* 5, 224–230.
- Syed, F., and Khosia, S. (2005). Mechanisms of sex steroid effects on bone. *Biochem. Biophys. Res. Commun.* 328, 688–696.
- Takeda, S., Eleftheriou, F., Levasseur, R., Liu, X., Zhao, L., Parker, K.L., Armstrong, D., Ducey, P., and Karsenty, G. (2002). Leptin regulates bone formation via the sympathetic nervous system. *Cell* 111, 305–317.
- Takezawa, S., Yokoyama, A., Okada, M., Fujiki, R., Iriyama, A., Yanagi, Y., Ito, H., Takada, I., Kishimoto, M., Miyajima, A., et al. (2007). A cell cycle-dependent co-repressor mediates photoreceptor cell-specific nuclear receptor function. *EMBO J.* 26, 764–774.
- Teitelbaum, S.L. (2006). Osteoclasts; culprits in inflammatory osteolysis. *Arthritis Res. Ther.* 8, 201.
- Teitelbaum, S.L. (2007). Osteoclasts: what do they do and how do they do it? *Am. J. Pathol.* 170, 427–435.
- Teitelbaum, S.L., and Ross, F.P. (2003). Genetic regulation of osteoclast development and function. *Nat. Rev. Genet.* 4, 638–649.
- Tolar, J., Teitelbaum, S.L., and Orchard, P.J. (2004). Osteopetrosis. *N. Engl. J. Med.* 351, 2839–2849.
- Windahl, S.H., Andersson, G., and Gustafsson, J.A. (2002). Elucidation of estrogen receptor function in bone with the use of mouse models. *Trends Endocrinol. Metab.* 13, 195–200.
- Yoshizawa, T., Handa, Y., Uematsu, Y., Takeda, S., Sekine, K., Yoshihara, Y., Kawakami, T., Arioka, K., Sato, H., Uchiyama, Y., et al. (1997). Mice lacking the vitamin D receptor exhibit impaired bone formation, uterine hypoplasia and growth retardation after weaning. *Nat. Genet.* 16, 391–396.
- Zaman, G., Jessop, H.L., Muzylak, M., De Souza, R.L., Pitsillides, A.A., Price, J.S., and Lanyon, L.L. (2006). Osteocytes use estrogen receptor alpha to respond to strain but their ERalpha content is regulated by estrogen. *J. Bone Miner. Res.* 21, 1297–1306.

#### Accession Numbers

Microarray can be seen in Gene Expression Omnibus under accession number GSE7798.

## A Novel Mechanism for Polychlorinated Biphenyl-Induced Decrease in Serum Thyroxine Level in Rats

Yoshihisa Kato, Shin-ichi Ikushiro, Rie Takiguchi, Koichi Haraguchi, Nobuyuki Koga, Shinya Uchida, Toshiyuki Sakaki, Shizuo Yamada, Jun Kanno, and Masakuni Degawa

Kagawa School of Pharmaceutical Sciences, Tokushima Bunri University, Sanuki, Kagawa, Japan (Y.K.); Faculty of Engineering, Toyama Prefectural University, Toyama, Japan (S.I., T.S.); School of Pharmaceutical Sciences and Center of Excellence (COE) Program in the 21<sup>st</sup> Century, University of Shizuoka, Shizuoka, Japan (R.T., S.U., S.Y., M.D.); Daiichi College of Pharmaceutical Sciences, Fukuoka, Japan (K.H.); Faculty of Nutritional Sciences, Nakamura Gakuen University, Fukuoka, Japan (N.K.); and Division of Cellular & Molecular Toxicology, National Institute of Health Sciences, Tokyo, Japan (J.K.)

Received June 19, 2007; accepted July 12, 2007

### ABSTRACT:

We have previously suggested that the decrease in the levels of serum total thyroxine ( $T_4$ ) and free  $T_4$  by a single administration to rats of Kanechlor-500 (KC500) at a dose of 100 mg/kg is not necessarily dependent on the increase in hepatic  $T_4$ -UDP-glucuronosyltransferase (UDP-GT). In the present study, we determined whether or not a consecutive treatment with KC500 at a relatively low dose (10 mg/kg i.p., once daily for 10 days) results in a decrease in the level of serum total  $T_4$  and further investigated an exact mechanism for the KC500-induced decrease in the  $T_4$ . At 4 days after final treatment with KC500, the serum total  $T_4$  and free  $T_4$  levels were markedly decreased in both Wistar and UGT1A-deficient Wistar (Gunn) rats, whereas significant increases in hepatic  $T_4$ -UDP-GT activity were observed in

Wistar rats but not in Gunn rats. The level of serum thyroid-stimulating hormone was not significantly changed in either Wistar or Gunn rats. Clearance from serum of the [ $^{125}$ I] $T_4$  administered to the KC500-pretreated Wistar and Gunn rats was faster than that to the corresponding control (KC500-untreated) rats. The accumulated level of [ $^{125}$ I] $T_4$  was increased in several tissues, especially the liver, in the KC500-pretreated rats. The present findings demonstrated that a consecutive treatment with KC500 resulted in a significant decrease in the level of serum total  $T_4$  in both Wistar and Gunn rats and further indicated that the KC500-induced decrease would occur through increase in accumulation of  $T_4$  in several tissues, especially the liver, rather than increase in hepatic  $T_4$ -UDP-GT activity.

Most polychlorinated biphenyls (PCBs) are known to decrease the level of serum thyroid hormone and to increase the activity of hepatic drug-metabolizing enzymes in rats (Van Birgelen et al., 1995; Craft et al., 2002). As possible mechanisms for the PCB-induced decrease in the level of serum thyroid hormone, enhancement of thyroid hormone metabolism by PCB and displacement of the hormone from serum transport proteins, including transthyretin (TTR), by PCB and its ring-hydroxylated metabolites are considered (Barter and Klaassen, 1992a, 1994; Brouwer et al., 1998). In particular, the decrease in the level of serum thyroxine ( $T_4$ ) by 3,3',4,4',5-pentachlorobiphenyl, Aroclor 1254, and 2,3,7,8-tetrachlorodibenzo-*p*-dioxin in rats is believed to occur mainly through induction of the UDP-glucuronosyltransferases (UDP-GTs), especially UGT1A subfamily enzymes, responsible for glucuronidation of  $T_4$  (Barter and Klaassen, 1994; Van Birgelen et al., 1995).

This work was supported in part by the Grant-in-Aid for Scientific Research (C) (no. 18510061; Y.K.) and for Scientific Research (B) (no. 19310042; K.H., Y.K.) from Japan Society for the Promotion of Science, and by a Health and Labour Sciences Research Grant for Research on Risk of Chemical Substances (H16-Kagaku-003; Y.K.) from the Ministry of Health, Labour and Welfare of Japan.

Article, publication date, and citation information can be found at <http://dmd.aspetjournals.org>.

doi:10.1124/dmd.107.017327.

However, the magnitude of decrease in the level of serum total  $T_4$  is not necessarily correlated with that of increase in  $T_4$ -UDP-GT activity (Craft et al., 2002; Hood et al., 2003). Furthermore, we have reported that in Kanechlor-500 (KC500)-treated mice, serum  $T_4$  level decreased without an increase in  $T_4$ -UDP-GT activity (Kato et al., 2003) and that the decrease in serum total  $T_4$  level by a single administration of either KC500 or 2,2',4,5,5'-pentachlorobiphenyl occurred even in UGT1A-deficient Wistar (Gunn) rats (Kato et al., 2004). Thus, an exact mechanism for the PCB-induced decrease in the level of serum thyroid hormone remains unclear. To date, most studies on biological effects of PCB have been performed using experimental animals treated once at a high dose (more than 100 mg/kg body weight), and the effect of the consecutive treatment at a low dose has been little reported. Humans and wild animals are exposed to a wide variety of environmental chemicals, including PCB, at a low level over a long period of time. Therefore, a study on biological effects by consecutive treatment with PCB at a low dose would be very important.

In the present study, therefore, we examined whether or not a consecutive treatment with KC500 at a relatively low dose (10 mg/kg i.p., once daily for 10 days) results in decrease in the level of serum total  $T_4$  and further discussed a mechanism underlying the PCB-induced decrease in the  $T_4$ .

**ABBREVIATIONS:** PCB, polychlorinated biphenyl; KC500, Kanechlor-500;  $T_3$ , triiodothyronine;  $T_4$ , thyroxine; TTR, transthyretin; TSH, thyroid-stimulating hormone; UDP-GT, UDP-glucuronosyltransferase.

Materials and Methods

**Chemicals.** Panacete 810 (medium-chain triglycerides) was purchased from Nippon Oils and Fats Co. Ltd. (Tokyo, Japan). The [<sup>125</sup>I]T<sub>4</sub>, radiolabeled at the 5'-position of the outer ring, was obtained from PerkinElmer Life and Analytical Sciences (Waltham, MA). The KC500 used in the present experiments contains 2,2',5,5'-tetrachlorobiphenyl (5.6% of total PCBs), 2,2',3,5',6-pentachlorobiphenyl (6.5%), 2,2',4,5,5'-pentachlorobiphenyl (10%), 2,3,3',4',6-pentachlorobiphenyl (7.4%), 2,3',4,4',5-pentachlorobiphenyl (7.7%), 2,2',3,4,4',5'-hexachlorobiphenyl (5.6%), and 2,2',4,4',5,5'-hexachlorobiphenyl (5.4%) as major PCB congeners (Haraguchi et al., 2005). All the other chemicals used herein were obtained commercially in appropriate grades of purity.

**Animal Treatments.** Male Wistar rats (160–200 g) and UGT1A-deficient Wistar rats (Gunn rats, 190–260 g) were obtained from Japan SLC, Inc. (Shizuoka, Japan). Male Wistar and Gunn rats were housed three or four per

cage with free access to commercial chow and tap water, maintained on a 12-h dark/light cycle (8:00 AM to 8:00 PM light) in an air-controlled room (temperature, 24.5 ± 1°C; humidity, 55 ± 5%), and handled with human care under the guidelines of the University of Shizuoka (Shizuoka, Japan). Rats received consecutive intraperitoneal injections of KC500 (10 mg/kg) dissolved in Panacete 810 (5 ml/kg) at 24-h intervals for 10 days. Control animals were treated with vehicle alone (5 mg/kg).

**In Vivo Study.** Rats were killed by decapitation 4 days after the final administration of KC500. The liver was removed, and hepatic microsomes were prepared according to the method of Kato et al. (1995) and stored at -85°C until use. Blood was collected from each animal between 10:30 and 11:30 AM. After clotting at room temperature, serum was separated by centrifugation and stored at -50°C until use.

TABLE 1

Effects of KC500 on the activity of hepatic microsomal alkoxyresorufin O-dealkylases in Wistar and Gunn rats

Animals were killed at 4 days after the final administration of KC500 (10 mg/kg i.p., once daily for 10 days). The values shown are expressed as the mean ± S.E. for four to five animals.

Substrates	Wistar		Gunn	
	Control	KC500	Control	KC500
	<i>nmol/mg protein/min</i>		<i>nmol/mg protein/min</i>	
7-Benzyloxyresorufin	0.07 ± 0.01	3.34 ± 0.33*	0.03 ± 0.003	1.08 ± 0.27*
7-Pentoxoresorufin	0.03 ± 0.003	0.43 ± 0.05*	0.02 ± 0.003	0.22 ± 0.05*
7-Ethoxyresorufin	0.14 ± 0.01	9.02 ± 0.09*	0.21 ± 0.01	2.21 ± 0.29*

\* P < 0.05, significantly different from each control.

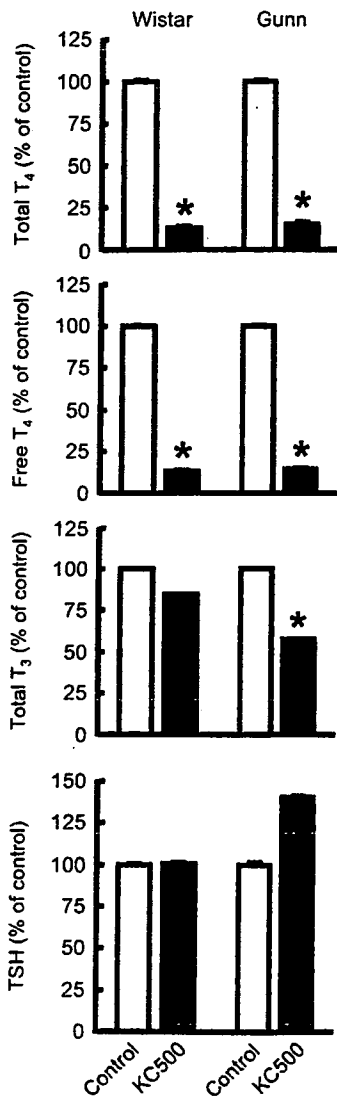


FIG. 1. Effects of KC500 on levels of serum total T<sub>4</sub>, free T<sub>4</sub>, total T<sub>3</sub>, and TSH in Wistar and Gunn rats. Animals were killed 4 days after the final administration of KC500 (10 mg/kg i.p., once daily for 10 days), and levels of serum thyroid hormones were measured as described under *Materials and Methods*. Constitutive levels: total T<sub>4</sub>, 4.29 ± 0.38 (Wistar, n = 5) and 5.80 ± 0.32 μg/dl (Gunn, n = 5); free T<sub>4</sub>, 2.17 ± 0.16 (Wistar, n = 5) and 2.71 ± 0.17 ng/dl (Gunn, n = 5); total T<sub>3</sub>, 0.34 ± 0.03 (Wistar, n = 6) and 0.96 ± 0.05 ng/ml (Gunn, n = 4); TSH, 4.89 ± 0.33 (Wistar, n = 5) and 7.48 ± 1.14 ng/ml (Gunn, n = 5). Each column represents the mean ± S.E. (vertical bars) for five to six animals. \*, P < 0.01, significantly different from each control.

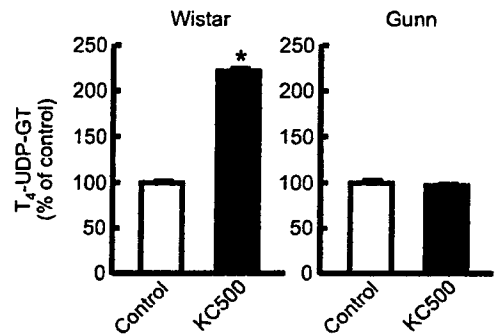


FIG. 2. Effects of KC500 on the activity of hepatic microsomal UDP-glucuronyltransferase in Wistar and Gunn rats. Each column represents the mean ± S.E. (vertical bars) for five to six animals. Constitutive levels: T<sub>4</sub>-UDP-GT, 14.17 ± 1.11 pmol/mg protein/min (Wistar) and 6.36 ± 1.34 pmol/mg protein/min (Gunn). \*, P < 0.01, significantly different from each control.

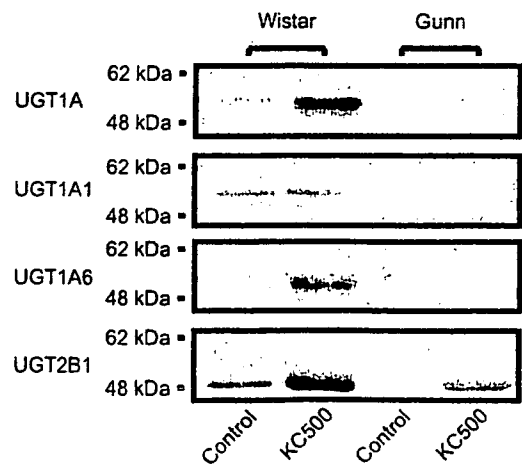


FIG. 3. Representative Western blot profiles for hepatic microsomal UGT isoforms in the KC500-treated Wistar and Gunn rats.

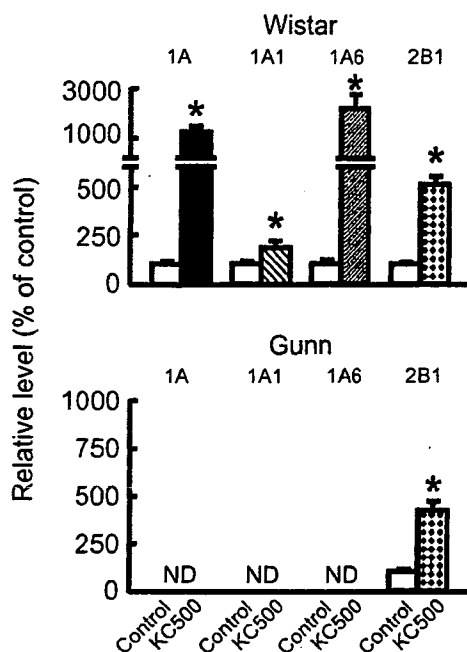


FIG. 4. Effects of KC500 on levels of hepatic microsomal UGT isoforms in Wistar and Gunn rats. The isolated bands responsible for UGT isoforms, which are shown in Fig. 3, were densitometrically quantified as described under *Materials and Methods*. The data are represented as the mean  $\pm$  S.E. (vertical bars) for five to six animals. \*,  $P < 0.05$ , significantly different from each control. ND, not detectable.

**Analysis of serum hormones.** Levels of total T<sub>4</sub>, free T<sub>4</sub>, total triiodothyronine (T<sub>3</sub>), and thyroid-stimulating hormone (TSH) were measured by radioimmunoassay using Total T<sub>4</sub> and Free T<sub>4</sub> kits (Diagnostic Products Corporation, Los Angeles, CA), the Triiodothyronine kit GammaCoat T<sub>3</sub> II (DiaSorin Inc., Stillwater, MN), and the rTSH [<sup>125</sup>I] Biotrak assay system (GE Healthcare UK, Ltd., Little Chalfont, Buckinghamshire, UK), respectively.

**Hepatic microsomal enzyme assays.** Hepatic microsomal fraction was prepared according to the method described previously (Kato et al., 1995), and the amount of hepatic microsomal protein was determined by the method of Lowry et al. (1951) with bovine serum albumin as a standard. Microsomal *O*-dealkylase activities of 7-benzoyloxy-, 7-ethoxy-, and 7-pentoxoresorufins were determined by the method of Burke et al. (1985).

**Hepatic T<sub>4</sub>-metabolizing enzyme assay.** The activity of microsomal UDP-GT toward T<sub>4</sub> (T<sub>4</sub>-UGT activity) was determined by the methods of Barter and Klaassen (1992b).

**Western blot analysis.** The polyclonal anti-peptide antibodies against the common region of UGT1A isoforms and specific antibodies against UGT1A1, UGT1A6, and UGT2B1, which were established by Ikushiro et al. (1995, 1997), were used. Western blot analyses for microsomal UGT isoforms were performed by the method of Luquita et al. (2001). The bands corresponding to UGT1A1, UGT1A6, and UGT2B1 on a sheet were detected using chemical luminescence (ECL detection kit; GE Healthcare UK, Ltd.), and the level of each protein was determined densitometrically with LAS-1000 (Fuji Photo Film Co., Ltd., Tokyo, Japan).

**Ex Vivo Study.** At 4 days after a consecutive 10-day treatment with KC500, the rats were anesthetized with a saline (2 ml/kg) containing sodium pentobarbital (25 mg/ml) and potassium iodide (1 mg/ml). The femoral artery was cannulated (polyethylene tube SP31; Natsume Inc., Tokyo, Japan) and primed with heparinized saline (33 units/ml), and then the animal's body was warmed to 37°C. Fifteen minutes later, the rats were given i.v. 1 ml of [<sup>125</sup>I]T<sub>4</sub> (15  $\mu$ Ci/ml) dissolved in the saline containing 10 mM NaOH and 1% normal rat serum.

**Clearance of [<sup>125</sup>I]T<sub>4</sub> from serum.** The study on the clearance of [<sup>125</sup>I]T<sub>4</sub> from serum was performed according to the method of Oppenheimer et al. (1968). In brief, after the administration of [<sup>125</sup>I]T<sub>4</sub>, a portion (0.3 ml) of blood was sampled from the artery at the indicated times, and serum was prepared and stored at -50°C until use. Two aliquots (15  $\mu$ l each) were taken from each

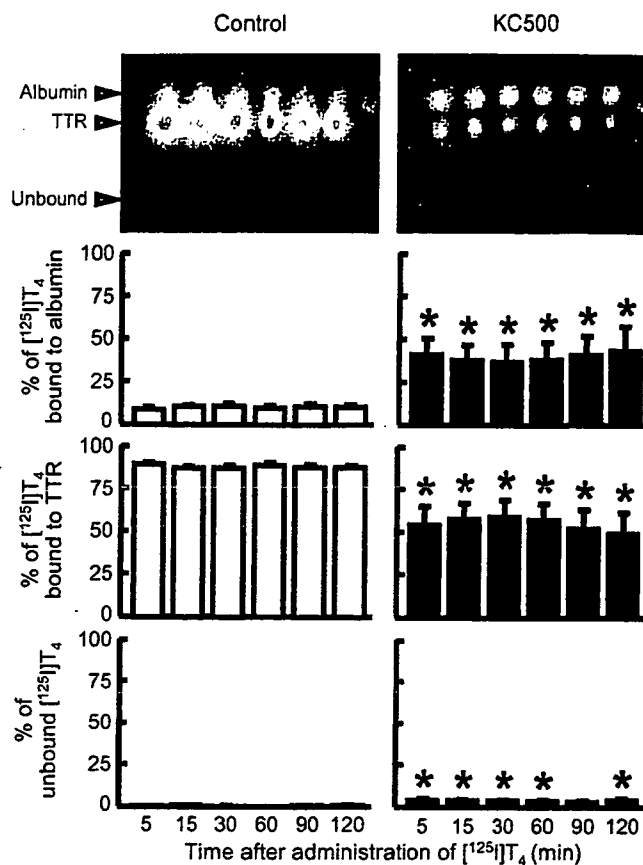


FIG. 5. Effects of KC500 on the binding of [<sup>125</sup>I]T<sub>4</sub> to serum proteins in Wistar rats. Amounts of [<sup>125</sup>I]T<sub>4</sub> bound to the serum proteins were assessed by the method described under *Materials and Methods*. Each column represents the mean  $\pm$  S.E. (vertical bars) for three to six animals. \*,  $P < 0.05$ , significantly different from each control.

serum sample for determining [<sup>125</sup>I]T<sub>4</sub> level by a gamma counter (COBRA II AUTO-GAMMA 5002; PerkinElmer Life and Analytical Sciences).

**Analysis of [<sup>125</sup>I]T<sub>4</sub> bound to serum proteins.** The levels of serum [<sup>125</sup>I]T<sub>4</sub>-albumin and [<sup>125</sup>I]T<sub>4</sub>-TTR complexes were determined according to the method of Davis et al. (1970). In brief, serum was diluted in 100 mM phosphate buffer (pH 7.4) containing 1 mM EDTA, 1 mM dithiothreitol, and 30% glycerol, and subjected to electrophoresis on 4 to 20% gradient native polyacrylamide gels PAG Mid "Daiichi" 4/20 (Daiichi Pure Chemicals Co., Ltd., Tokyo, Japan). The electrophoresis was performed at 4°C for 11 h at 20 mA in the 0.025 M Tris buffer (pH 8.4) containing 0.192 M glycine. The human albumin and TTR, which were incubated with [<sup>125</sup>I]T<sub>4</sub>, were also applied on the gel as templates. After the electrophoresis, a gel was dried and radioautographed for 20 h at room temperature using Imaging Plate 2040 (Fuji Photo Film Co., Ltd.). The levels of [<sup>125</sup>I]T<sub>4</sub>-albumin and [<sup>125</sup>I]T<sub>4</sub>-TTR in serum were determined by counting the gel fractions identified from Bio Imaging Analyzer (BAS-2000II IP Reader; Fuji Photo Film Co., Ltd.).

**Tissue distribution of [<sup>125</sup>I]T<sub>4</sub>.** The study on the tissue distribution of [<sup>125</sup>I]T<sub>4</sub> was performed according to the modified method of Oppenheimer et al. (1968). In brief, at 60 min after administration of [<sup>125</sup>I]T<sub>4</sub> to KC500-pretreated rats, blood was sampled from abdominal aorta. Then, cerebrum, cerebellum, pituitary gland, thyroid gland, sublingual gland, submandibular gland, thymus, heart, lung, liver, kidney, adrenal gland, spleen, pancreas, testis, prostate gland, seminal vesicle, stomach, duodenum, jejunum, ileum, cecum, brown fat, skeletal muscle, bone marrow, skin, spinal cord, and fat were removed and weighed. Radioactivities in serum and the tissues were determined by a gamma-counter (COBRA II AUTO-GAMMA5002; PerkinElmer Life and Analytical Sciences), and amounts of [<sup>125</sup>I]T<sub>4</sub> in various tissues were shown as ratios of tissue to serum.

**Statistics.** The data obtained were statistically analyzed according to Stu-

dent's *t* test or Dunnett's test after analysis of variance. In addition, data of the clearance of [<sup>125</sup>I]T<sub>4</sub> from serum and analysis of [<sup>125</sup>I]T<sub>4</sub> bound to serum proteins were statistically analyzed according to the Newman-Keuls test after analysis of variance. The pharmacokinetic parameters of [<sup>125</sup>I]T<sub>4</sub> were estimated with noncompartmental methods as described previously (Tabata et al., 1999).

**Results**

**Serum Hormone Levels.** Effects of KC500 on levels of serum thyroid hormones were examined in Wistar and Gunn rats (Fig. 1). In both Wistar and Gunn rats, KC500 treatment resulted in decreases of the serum total T<sub>4</sub> and free T<sub>4</sub>, and the magnitude of the decrease in each serum thyroid hormone was almost the same in both strains of rats. On the other hand, a significant decrease in the level of serum total T<sub>3</sub> was observed in Gunn rats but not in Wistar rats. In addition,

no significant change in TSH level was observed in either Wistar or Gunn rats.

**Hepatic Drug-Metabolizing Enzymes.** Effects of KC500 on hepatic microsomal activities of benzyloxyresorufin *O*-dealkylase (CYP2B1/2 and CYP3A1/2), pentoxyresorufin *O*-dealkylase (CYP2B1/2), and ethoxyresorufin *O*-dealkylase (CYP1A1/2) were examined in Wistar and Gunn rats. In both Wistar and Gunn rats, these enzyme activities were significantly increased by KC500 (Table 1), and the increase in each enzyme activity was much greater in Wistar rats than in Gunn rats.

**Hepatic T<sub>4</sub>-Metabolizing Enzyme Activities.** T<sub>4</sub> glucuronidation is primarily mediated by hepatic T<sub>4</sub>-UDP-GTs, such as UGT1A1 and UGT1A6, in the rat liver (Visser, 1996), and a chemical-mediated induction of the enzymes is considered to contribute to the decrease in the level of serum total T<sub>4</sub>. Therefore, we examined effects of KC500 on hepatic microsomal T<sub>4</sub>-UDP-GT activity in Wistar and Gunn rats. Constitutive activity of T<sub>4</sub>-UDP-GT was approximately 2.2-fold higher in Wistar rats than in Gunn rats. Treatment with KC500 resulted in significant increase of T<sub>4</sub>-UDP-GT activity in Wistar rats but not in Gunn rats (Fig. 2).

**Western Blot Analysis for UGT1As.** Levels of the proteins responsible for UGT1A enzymes, UGT1A1 and UGT1A6, were increased by KC500 treatment in Wistar rats but not in Gunn rats (Figs. 3 and 4). In addition, no expression of the UGT1A enzymes was confirmed in Gunn rats. On the other hand, the level of UGT2B1 was significantly increased by KC500 in both Wistar and Gunn rats, and magnitudes of the increase in both strains of rats were almost the same (Figs. 3 and 4).

**Serum Proteins Bound to [<sup>125</sup>I]T<sub>4</sub>.** The effects of KC500 on the binding of [<sup>125</sup>I]T<sub>4</sub> to serum proteins, TTR, and albumin were examined in Wistar and Gunn rats (Figs. 5 and 6). In both Wistar and Gunn rats, pretreatment with KC500 resulted in a significant decrease in the level of [<sup>125</sup>I]T<sub>4</sub>-TTR complex, whereas it resulted in a significant increase in the level of [<sup>125</sup>I]T<sub>4</sub> bound to albumin (Figs. 5 and 6).

**Clearance of [<sup>125</sup>I]T<sub>4</sub> from Serum.** After an i.v. administration of [<sup>125</sup>I]T<sub>4</sub> to the KC500-pretreated Wistar and Gunn rats, concentrations of [<sup>125</sup>I]T<sub>4</sub> in sera were measured at the indicated times (Fig. 7). In both Wistar and Gunn rats, pretreatment with KC500 promoted the clearance of [<sup>125</sup>I]T<sub>4</sub> from serum, and their serum [<sup>125</sup>I]T<sub>4</sub> levels were decreased to approximately 40% of the initial level within 5 min. In the KC500-untreated Wistar and Gunn rats, serum [<sup>125</sup>I]T<sub>4</sub> levels were gradually decreased to approximately 40% of the initial level at 120 min later. The serum pharmacokinetic parameters of the [<sup>125</sup>I]T<sub>4</sub> estimated from these data (Fig. 7) were summarized in Table 2. The mean total body clearances (CL<sub>tb</sub>) of [<sup>125</sup>I]T<sub>4</sub> in the KC500-pretreated rats were 2.4 and 2.9 times, respectively, greater than those in the corresponding control rats. The steady-state volumes of distribution (Vd<sub>ss</sub>) in the KC500-pretreated rats were 1.6 and 2.4 times, respectively, larger than those in the corresponding control rats.

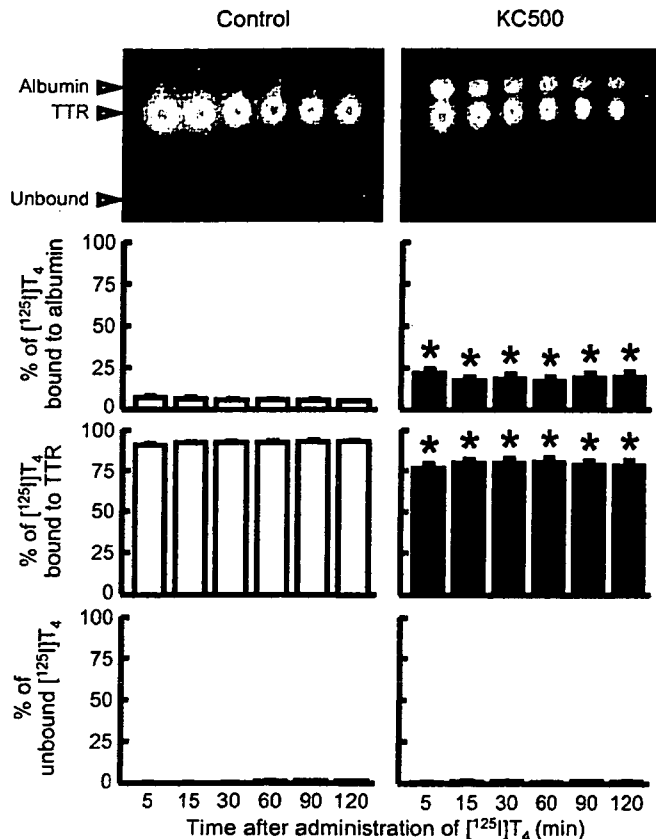


FIG. 6. Effects of KC500 on the binding of [<sup>125</sup>I]T<sub>4</sub> to serum proteins in Gunn rats. Amounts of [<sup>125</sup>I]T<sub>4</sub> bound to the serum proteins were assessed by the method described under *Materials and Methods*. Each column represents the mean ± S.E. (vertical bars) for four to five animals. \*, *P* < 0.05, significantly different from each control.

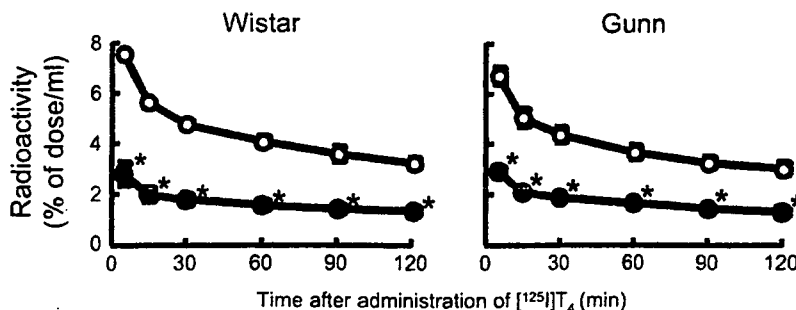


FIG. 7. Effects of KC500 on the clearance of [<sup>125</sup>I]T<sub>4</sub> from serum in Wistar and Gunn rats. The amount of serum [<sup>125</sup>I]T<sub>4</sub> was measured at the indicated times after the i.v. administration of [<sup>125</sup>I]T<sub>4</sub>. Each point represents the mean ± S.E. (vertical bars) for four to eight animals. \*, *P* < 0.001, significantly different from each control. ○, control; ●, KC500.

**Tissue Distribution of [<sup>125</sup>I]T<sub>4</sub>.** The tissue-to-serum concentration ratio ( $K_p$  value) and distribution level of [<sup>125</sup>I]T<sub>4</sub> in tissue after the administration of [<sup>125</sup>I]T<sub>4</sub> to the KC500-pretreated Wistar and Gunn rats are shown in Figs. 8 and 9, respectively.  $K_p$  values of the thyroid gland and liver were the greatest among those of the tissues examined in either Wistar or Gunn rats (Fig. 8). In addition,  $K_p$  values in all the tissues examined, with the exception of the testis and ileum, were greater in KC500-pretreated Wistar rats than those in the corresponding control (KC500-untreated) rats.  $K_p$  values in the thyroid gland, liver, and jejunum in the KC500-pretreated Wistar and Gunn rats were 1.6 to 1.8, 3.3 to 3.8, and 4.7 to 11.5 times, respectively, higher than those in corresponding control rats (Fig. 8).

In the control Wistar and Gunn rats, the accumulation level of [<sup>125</sup>I]T<sub>4</sub> was highest in the liver, among the tissues examined (Fig. 9). In both Wistar and Gunn rats, pretreatment with KC500 resulted in an increase in the accumulation level in the liver, and the levels increased to more than 40% of the [<sup>125</sup>I]T<sub>4</sub> dosed (Fig. 9). Likewise, significant increase in accumulation of [<sup>125</sup>I]T<sub>4</sub> was observed in the jejunum (Fig. 9). In addition, significant increases in the liver weight and accumulation level (per g liver) of [<sup>125</sup>I]T<sub>4</sub> occurred in KC500-pretreated Wistar rats, but not in Gunn rats (Tables 3 and 4).

### Discussion

In the present study, we found that consecutive treatment with KC500 (10 mg/kg i.p., once daily for 10 days; total dose, 100 mg/kg) promoted accumulation of T<sub>4</sub> in several tissues, especially the liver, and resulted in a drastic decrease in the levels of serum total T<sub>4</sub> and

free T<sub>4</sub> in both Wistar and Gunn (UGT1A-deficient) rats. Thus, a decrease in the level of serum total T<sub>4</sub> is also observed in the Wistar and Gunn rats treated with KC500 (a single i.p. administration at a dose of 100 mg/kg) (Kato et al., 2004). In addition, constitutive levels of serum total T<sub>4</sub> and T<sub>3</sub> were higher in Gunn rats than in Wistar rats, and the results were identified with those as previously described by Benathan et al. (1983). The difference in constitutive level of serum thyroid hormone between Wistar and Gunn rats seems to be dependent on differences in the level and/or activity of T<sub>4</sub>/T<sub>3</sub>-UDP-GTs.

As a possible explanation for a chemical-induced decrease in serum thyroid hormones, a hepatic T<sub>4</sub>-UDP-GT-dependent mechanism is generally considered, because T<sub>4</sub>-UDP-GT inducers, including PCB, phenobarbital, 3-methylcholanthrene, pregnenolone-16 $\alpha$ -carbonitrile, and clobazam, show strong activities for decreasing the level of serum total thyroid hormones, including T<sub>4</sub> and T<sub>3</sub> (Barter and Klaassen, 1994; Van Birgelen et al., 1995; Miyawaki et al., 2003). However, among the experimental animals treated with a T<sub>4</sub>-UDP-GT inducer, the difference in magnitude of decrease in the level of serum total T<sub>4</sub> is not necessarily correlated with that of hepatic T<sub>4</sub>-UDP-GT activity (Craft et al., 2002; Hood et al., 2003; Kato et al., 2003). Our present and previous results (Kato et al., 2004, 2005) using Wistar and Gunn rats support a hypothesis that significant decrease in the level of serum total thyroid hormones by either PCB or phenobarbital occurs primarily in a hepatic T<sub>4</sub>-UDP-GT-independent pathway.

As a possible mechanism for the PCB-induced decrease in serum T<sub>4</sub> level, an increase in hepatic drug-metabolizing enzymes might be considered. However, these are induced to a greater extent in the Wistar rats than in the Gunn rats, whereas magnitudes of decrease in serum T<sub>4</sub> level in Wistar and Gunn rats were almost the same. Accordingly, the KC500-induced decrease in serum T<sub>4</sub> level is thought to be independent of the KC500-induced drug-metabolizing enzymes, including UDT-GTs and cytochromes P450.

As the factors regulating the level of serum total T<sub>4</sub>, serum TSH, hepatic type I iodothyronine deiodinase, and TTR are known. However, no significant change in the level of serum TSH occurs in the PCB-treated rats (Liu et al., 1995; Hood et al., 1999; Hallgren et al., 2001; Kato et al., 2004). Hepatic type I iodothyronine deiodinase activity was significantly decreased in Wistar and Gunn rats by KC500 (Kato et al., 2004). On the other hand, a TTR-associated pathway might be considered as an explanation for the PCB-induced decrease in the level of serum total

TABLE 2

Pharmacokinetic parameters for [<sup>125</sup>I]T<sub>4</sub> after the administration of [<sup>125</sup>I]T<sub>4</sub> to the KC500-pretreated Wistar and Gunn rats

The experimental conditions were the same as those described in Fig. 7. The values shown are expressed as the mean  $\pm$  S.E. for four to seven animals.

Animal	Treatment	Mean Total Body Clearance $\times$ 100	Distribution Volume
		ml/min	ml
Wistar	Control	7.82 $\pm$ 0.59	17.91 $\pm$ 0.52
	KC500	18.85 $\pm$ 3.49*	51.51 $\pm$ 6.34*
Gunn	Control	8.44 $\pm$ 0.22	20.21 $\pm$ 1.79
	KC500	13.84 $\pm$ 0.88*	48.91 $\pm$ 3.50*

\*  $P < 0.05$ , significantly different from each control.

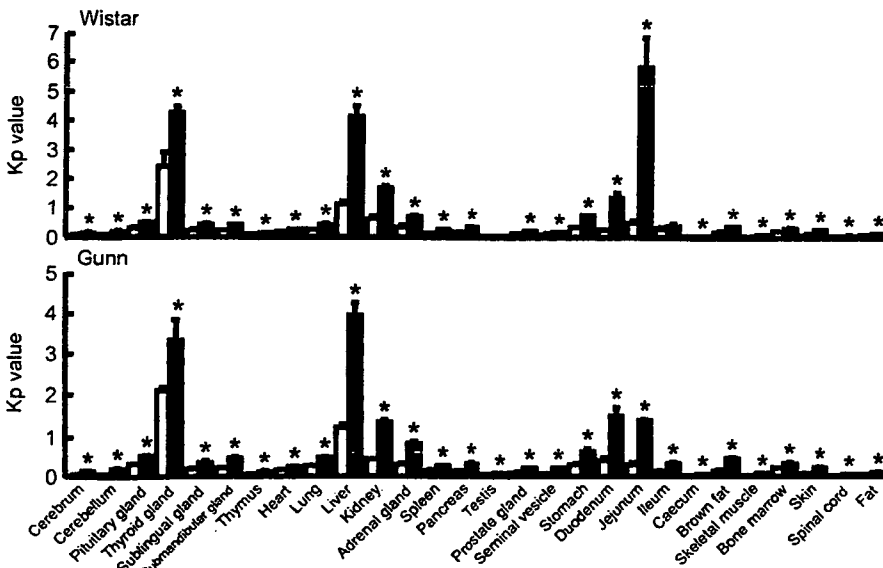


FIG. 8. Tissue-to-serum concentration ratio ( $K_p$  value) of [<sup>125</sup>I]T<sub>4</sub> in various tissues after administration of [<sup>125</sup>I]T<sub>4</sub> to the KC500-pretreated Wistar and Gunn rats. KC500 (10 mg/kg) was given i.p. to animals once daily for 10 days, and then, the animals were administered i.v. [<sup>125</sup>I]T<sub>4</sub>. At 60 min after administration of [<sup>125</sup>I]T<sub>4</sub>, the radioactivity in each tissue was measured. Each column represents the mean  $\pm$  S.E. (vertical bars) for three to six animals. \*,  $P < 0.05$ , significantly different from each control. □, control; ■, KC500.

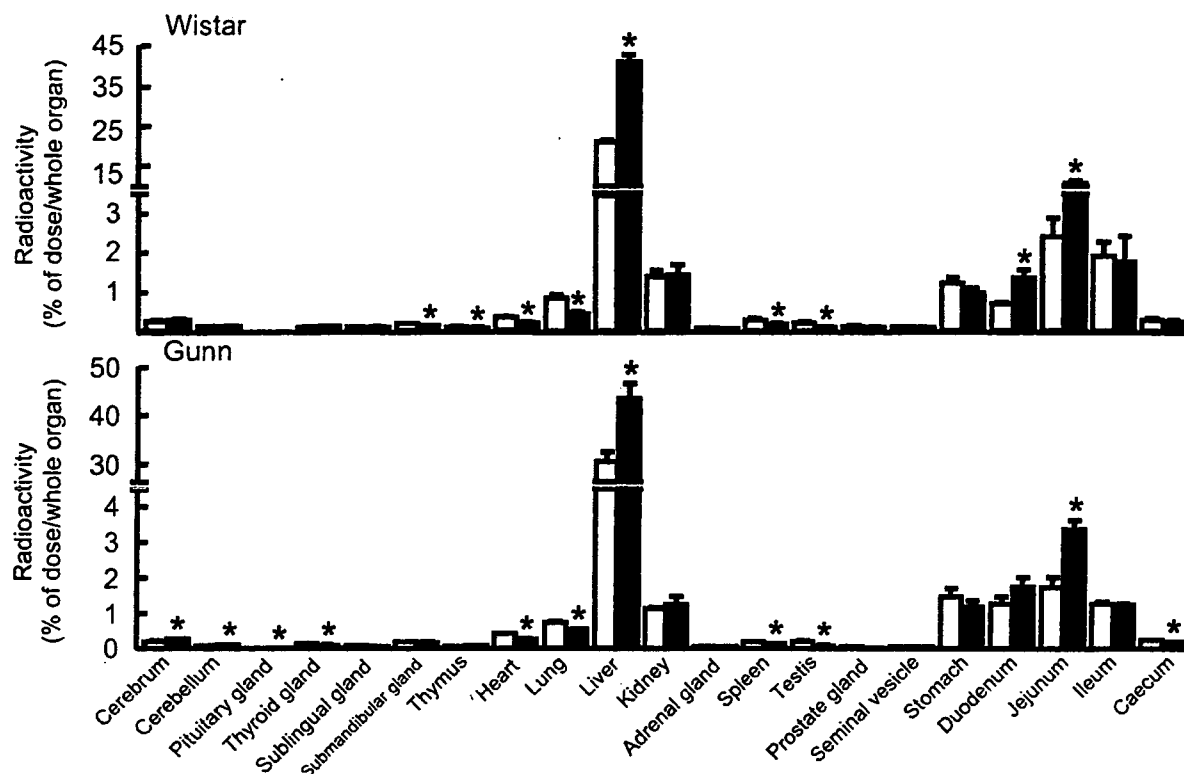


Fig. 9. Tissue distribution of [ $^{125}\text{I}$ ] $\text{T}_4$  after administration of [ $^{125}\text{I}$ ] $\text{T}_4$  to the KC500-pretreated Wistar and Gunn rats. The experimental conditions were the same as those described in Fig. 8. Each column represents the mean  $\pm$  S.E. (vertical bars) for four to six animals. \*,  $P < 0.05$ , significantly different from each control.  $\square$ , control;  $\blacksquare$ , KC500.

TABLE 3

*Liver weights after the administration of KC500 to Wistar and Gunn rats*

Animals were killed at 4 days after the final administration of KC500 (10 mg/kg i.p., once daily for 10 days). The values shown are expressed as the mean  $\pm$  S.E. for four to six animals.

Animal	Liver Weight	
	Control	KC500
	% of body weight	
Wistar	3.07 $\pm$ 0.04	3.81 $\pm$ 0.17*
Gunn	3.25 $\pm$ 0.08	3.38 $\pm$ 0.10

\* $P < 0.01$ , significantly different from each control.

TABLE 4

*Accumulation of [ $^{125}\text{I}$ ] $\text{T}_4$  in the KC500-pretreated Wistar and Gunn rat livers*

The experimental conditions were the same as those described in Fig. 8. The values shown are expressed as the mean  $\pm$  S.E. for four to six animals.

Animal	[ $^{125}\text{I}$ ] $\text{T}_4$	
	Control	KC500
	% of dose/g liver	
Wistar	3.86 $\pm$ 0.18	6.01 $\pm$ 0.24*
Gunn	4.74 $\pm$ 0.43	6.33 $\pm$ 0.62

\* $P < 0.001$ , significantly different from each control.

$\text{T}_4$ , because PCB and its ring-hydroxylated metabolites act as  $\text{T}_4$  antagonists to TTR (Lans et al., 1993; Brouwer et al., 1998; Meerts et al., 2002; Kato et al., 2004). Thus, competitive inhibition by PCB and/or its metabolites would promote a decrease in the level of serum total  $\text{T}_4$ . In the present study, significant decrease in the level of [ $^{125}\text{I}$ ] $\text{T}_4$  bound to serum TTR and increase in the level of [ $^{125}\text{I}$ ] $\text{T}_4$  bound to serum albumin

occurred in both KC500-pretreated Wistar and Gunn rats, suggesting that PCB and/or its metabolite(s) inhibit the formation of serum  $\text{T}_4$ -TTR complex.

Thus, inhibition of the  $\text{T}_4$ -TTR formation might lead to change in the tissue distribution of  $\text{T}_4$ . Therefore, to clarify this, we administered [ $^{125}\text{I}$ ] $\text{T}_4$  to KC500-pretreated Wistar and Gunn rats and, thereafter, determined the levels of [ $^{125}\text{I}$ ] $\text{T}_4$  in their tissues. In addition, since [ $^{125}\text{I}$ ] $\text{T}_4$  in either plasma or tissues is known to be stable during 48 h (Oppenheimer et al., 1968), the radioactivity detected in the serum and tissues would be attributed to [ $^{125}\text{I}$ ] $\text{T}_4$  in each tissue. Marked increases in the mean total body clearance of [ $^{125}\text{I}$ ] $\text{T}_4$  and in the steady-state distribution volume of [ $^{125}\text{I}$ ] $\text{T}_4$  were observed in the KC500-pretreated rats. A tissue-to-serum concentration ratio ( $K_p$  value) was greater in several tissues, especially the liver, of the KC500-pretreated Wistar and Gunn rats than in the corresponding control (KC500-untreated) rat tissues. In addition, in both KC500-pretreated Wistar and Gunn rats, more than 40% of the [ $^{125}\text{I}$ ] $\text{T}_4$  dosed was accumulated in the liver.

In conclusion, the present findings confirmed that PCB-induced decrease in serum  $\text{T}_4$  occurs not only in Wistar rats but also in Gunn (UGT1A-deficient) rats and further led to a hypothesis that the PCB-induced decrease occurs through increase in accumulation (transportation from serum to liver) of  $\text{T}_4$  in the liver, rather than through induction of hepatic  $\text{T}_4$ -UDP-GT. In addition, the increased accumulation in the liver might be attributed to the PCB- and its metabolite(s)-mediated inhibition of formation of serum  $\text{T}_4$ -TTR complex.

#### References

- Barter RA and Klaassen CD (1992a) UDP-glucuronosyltransferase inducers reduce thyroid hormone levels in rats by an extrathyroidal mechanism. *Toxicol Appl Pharmacol* 113:36-42.  
Barter RA and Klaassen CD (1992b) Rat liver microsomal UDP-glucuronosyltransferase activity